iJRASET
International Journal For Research in Applied Science and Engineering Technology



# INTERNATIONAL JOURNAL FOR RESEARCH

IN APPLIED SCIENCE & ENGINEERING TECHNOLOGY

**Volume:** 10 **Issue:** V **Month of publication:** May 2022

**DOI:** https://doi.org/10.22214/ijraset.2022.43169

www.ijraset.com

Call: 08813907089 | E-mail ID: ijraset@gmail.com

International Journal for Research in Applied Science & Engineering Technology (IJRASET)
*ISSN: 2321-9653; IC Value: 45.98; SJ Impact Factor: 7.538*
*Volume 10 Issue V May 2022- Available at www.ijraset.com*

# Design and Analysis of Hybrid Turbocharger

Kaiwalya Labade[1], Tanmay Pawar[2], Abhishek Patil[3], Rishikesh Ware[4]
[1, 2, 3, 4]*Mechanical Dept. K.K.W.I.E.E.R*

***Abstract:*** ***Internal Combustion engines have the capacity to exploit its increase in performance. Part ofwhich can be boosted by the technical solution that is turbocharging. To optimize the turbocharging to react as fast as possible and to adjust the volumetric flow of exhaust gases in the turbine, different alterations to turbochargers are done. To optimally support downsizing of Internal Combustion engines, these alterations are necessary.***
***In a VGT there are vanes on the compressor that change the A/R of the turbo as needed. VGTs show a great improvement over conventional single turbocharger. Sequential turbocharger has an edge over VGT, but they are much more complicated. A 2.2L sequential turbocharged engine is same in performance as a 2.7L VGT engine. Exhaust gas turbocharging is a major technology for reducing fuel consumption and emissions in internal combustion engines, improving engine performance while cutting CO2 emissions. There are also electric turbochargers that almost totally eliminate turbo lag by using a motor to spin the compressor and use a generator on the turbine to recover exhaust gas energy. This application reduces fuel usage by up to 5% for driving cycles. EATC reduced the time it took to reach the optimum boost level during a load increase by up to 30%.***
***Turbocharging is a major technology for reducing fuel consumption and emissions in internal combustion engines, improving engine performance while cutting CO2 emissions. Hybrid Turbocharging application leads to remarkable improvement at low-end torques, better engine performance and increased overall engine efficiency which paves way for downsizing of Internal Combustion engines.***
***Keywords: Internal Combustion Engine, Hybrid turbocharger, Turbo-lag, VGTs.***

## I. INTRODUCTION

The goal of automotive research has always been to build high-performance engines with improved dynamic responsiveness regardless of the driving circumstances. A turbocharger, or turbo, is a turbine-driven forced induction device that boosts the efficiency and power output of an internal combustion engine by forcing more compressed air into the combustion chamber.

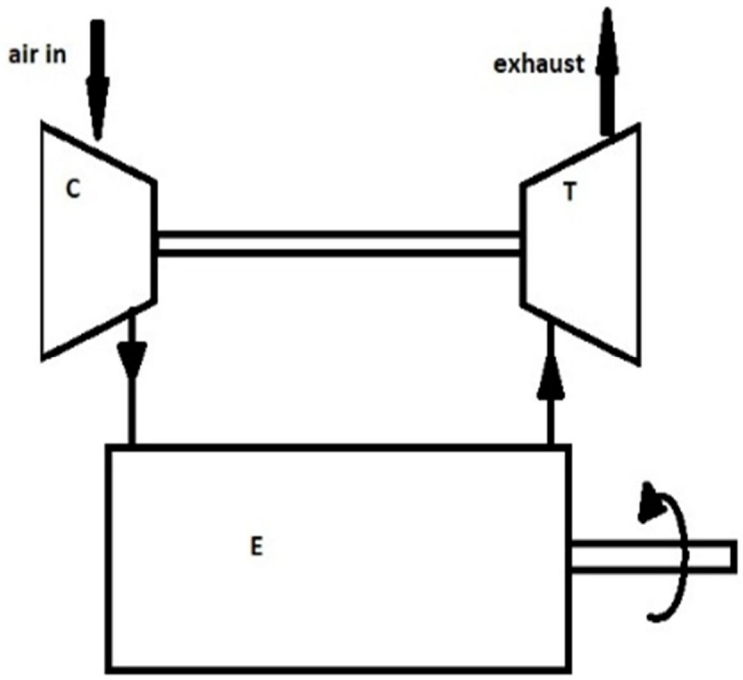



Fig (1.1): Single Turbo

©IJRASET: All Rights are Reserved 

More the compressed air forced into the chamber, more effectively fuel is burnt. Resulting maximum engine's power. The amount of fuel injected is determined by the amount of air available at each cycle. As a result, compressing air to a greater density allows more air to enter the cylinder.

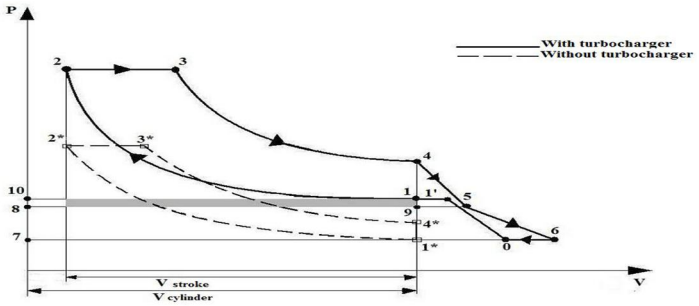



Fig (1.2): Turbocharger Cycle

This graph mainly differs the charged air system of conventional diesel cycle with and without turbocharger.
1-2: Isentropic compression at constant pressure.
2-3: Constant volume heat addition
3-4: Isentropic expansion
4-1: Constant volume heat rejection.
However, the cycle continues in turbocharged engine,
4-5: Exhaust gas expands through turbine inlet
5-6: Hot air expands to atmospheric pressure
The expansion of hot air converts heat energy to kinetic energy, which is transferred to compressor wheel.
6-0: Compressor sucks air from environment and compress it.
1'-1: Compressed and heated air enters the intercooler and enters the cylinder.
'Grey Area': Pumping Mean Effective Work.

Turbocharged engines provide a number of advantages over normally aspirated engines or we can say naturally aspirated engines, but they also have certain drawbacks. One of them is a more costly and intricate engine design, as well as decreased dependability. These drawbacks can be nullified to some extent. Variable Geometry Turbochargers (VGTs). VG turbochargers are a type of turbochargers that allows the effective aspect ratio (A: R) of the turbo to be changed as conditions change. Because the optimal aspect ratio at low engine speeds differs significantly from that at high engine speeds, this is done. When VGT, fitted to a 7.8L V8 CI truck by Gravdal et al. [8], showed a 2-second improvement over a normal turbocharger
Electric motor is used to increase the overall performance of a turbocharged IC engine. Beyond the efficiency of a typical turbocharger, this design flexibility leads to even greater increases in turbine and compressor efficiency. A hybrid turbocharging assist system is a potential technique for boosting engine economy while also enhancing transient responsiveness. This application reduces fuel usage by up to 5% for driving cycles. EATC reduced the time it took to reach the optimum boost level during a load increase by up to 30%, as experimented by Gravdal et al. [8].

### *A. Problem Statement*

The issue is reducing the transient response time of the engine, commonly known as turbo lag, which affects the initial acceleration of the engine. In addition, the materials used for the turbines can be improved.

### *B. Objectives*

*1)* To study how turbochargers function so that their performance can be improved
*2)* Study the effect of turbocharger geometry on engine performance.
*3)* Find out how to select an efficient turbocharger for a given engine.
*4)* Study of different types of materials used for turbochargers.

## II. LITERATURE REVIEW

Chiriac et al. [1] in his research found that the turbocharger has a high working potential and may be used with a generator without lowering the turbocharger or the internal combustion engine's efficiency. The findings of generating 115 W of electrical power with a turbocharger shaft speed of 140,000–160,000 rpm and an electric generator shaft speed of 14,000–16,000 rpm is presented in detail in this study. The loss of mechanical power of the turbocharger owing to the connected gearbox and generator is a weakness of this study. Friction is created by them, and this is the primary source of power losses. Finally, no electrical or mechanical losses, such as the alternator, gear ratio, or shaft transmission, are considered in any of the data reported in this study, which will certainly diminish the net quantity of captured energy.

Capata et al. [2] did the current study, which is part of a larger research effort, that concerns the reworking of an existing turbocharger unit in a 998 gasoline-powered city automobile. The proposed solution is to physically separate the compressor and turbine, with the former being powered by an electric motor and the latter being collected by an electric generator. Both machines were rebuilt to enhance surge and choke characteristics, with the compressor being increased in size. Complete simulations of both machines, which were given elsewhere, also showed higher efficiency and supplied operating curves for the current work. The extra power was computed using a challenging mission profile: the total energy recovered for the full voyage is 1.01 kWh (against the 18 kWh of total energy used by the vehicle), implying a net save of around 5.6 percent by installing the unique turbocharger unit.

Rares-Lucian Chiriac et al. [3] in his research paper focuses on the new technical solution for hybrid turbochargers. The study resulted of the hybrid turbocharger's experimental study, to simulate and test novel methods for improving the energy performance of internal combustion engines utilizing hybrid turbochargers with a linked electric generator. Simulations were performed using Siemens' AMESim software to show the efficiency of innovative solutions such as a hybrid turbocharger through calculations. A peak of 23 Volt and 4.2 Ampere was generated from the electric motor at running at 164200 rpm under 1bar of pressure.

Bhavik Kumar Padhiyar et al. [4] describes the application of hybrid turbocharger to improve performance of engine. It was stated a mixture ratio of 2.2 lbs. fuel and approximately 33 lbs. air is required in the engine to achieve good and complete combustion. Exhaust gas turbocharging is a significant method for reducing fuel consumption and emissions in internal combustion engines, resulting in improved engine performance and decreased CO2 emissions.

Nenad Raspopović et al. [5] emphasizes on Analysis of hybrid turbocharger in motor vehicle IC engine. The possibility of utilizing an electric motor to give direct power to the crankshaft was investigated, as well as the practicality of the solution and how it affects the compressor's operation. An approx. increase of 6.1% increase was seen in the brake power, and 4.26% in brake torque was seen.

Alin-Gabriel, D. et al. [6] refers to the possibility of implementing a hybrid turbocharging assisting system on a VEP 2.0 L engine. Two modules are studied: electrically assistance for the turbocharger which regards the transient performance and exhaust gas energy recovery which regards the engine efficiency. An electric machine is connected to the turbocharger's shaft through a planetary gear, enabling two operating modes: motor in electrical assistance and generator in energy recovery mode. Transient simulations are performed for the electrical assistance module having three configurations: a standard and a bigger compressor (HP Compressor) and a bigger turbine (HP Turbine). The results of the electrically assisted module reveal that employing the normal compressor design improves transient performance by 30% at 1400 rpm, 20% at 1600 rpm, and 16% at 1800 rpm. When implementing an exhaust gas energy recovery system, a larger turbine arrangement improves engine efficiency dramatically.

### *A. Inference from Literature Review*

*1)* Different types of turbochargers such as variable geometry turbocharger, sequential turbocharger and electrically assisted turbocharger, show significant improvement in terms of turbo lag.

*2)* During a transient, a VGT can be actively managed to achieve beneficial flow characteristics. From standstill until the end of first gear, where the turbo-lag effects are most noticeable, a 2-second improvement over a normal turbocharger can be noted.

*3)* The turbocharger has a high working potential and may be linked with a generator without lowering the turbocharger's or the internal combustion engine's efficiency.

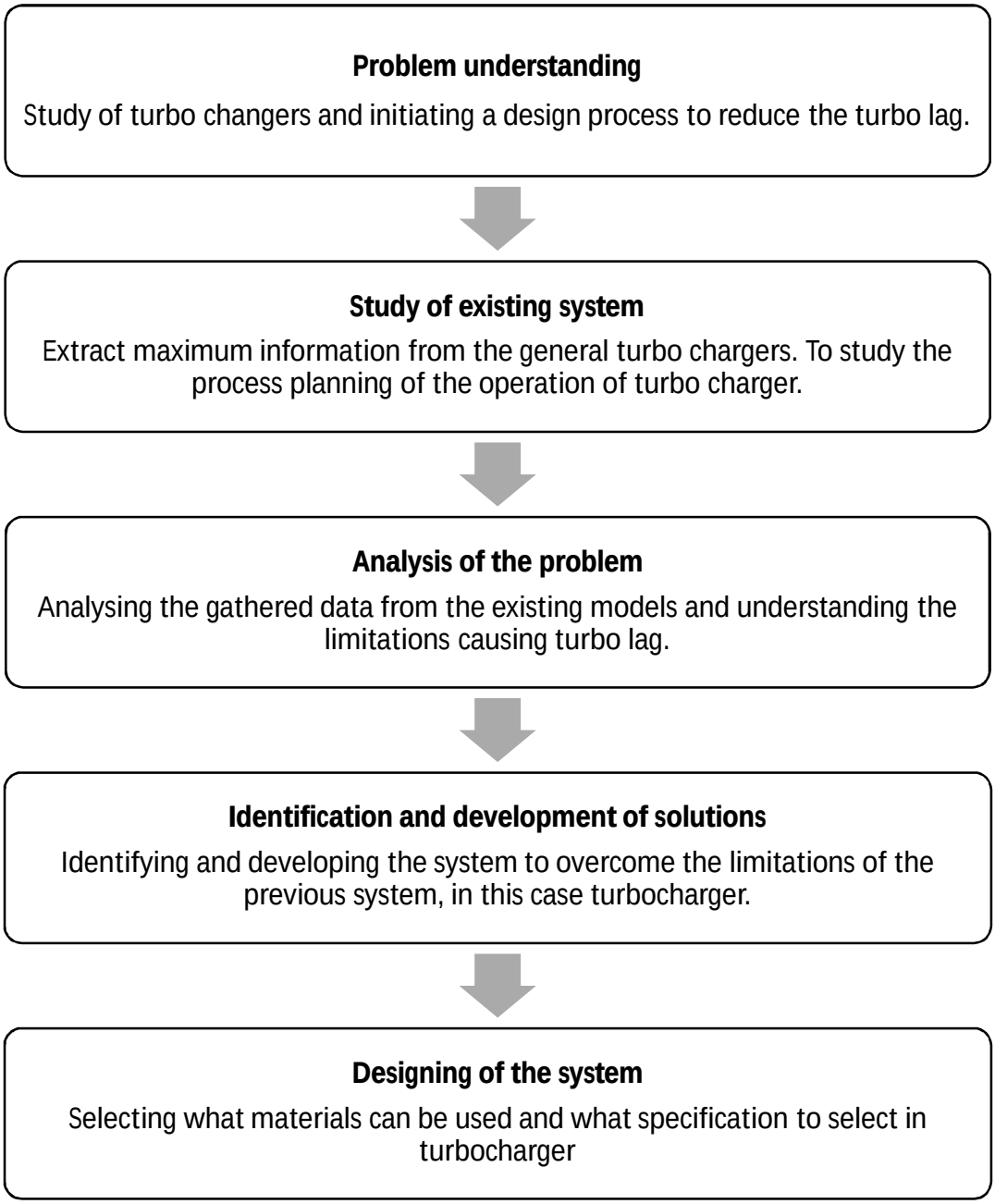
*4)* With the help of turbochargers, we can push more air into the engine, which creates a denser air fuel ratio resulting in more power generated from the combustion. This can help with downsizing of an engine. Sequential turbochargers seem to be more effective than VGTs because they have two turbos working at the same time and can help in downsizing an engine significantly.

*5)* EATC give the best results when comparing response time of the TC. The amount of torque and power delivered can be increased or decreased by using an appropriately powered motor. But using a more powerful motor results in a much expensive setup.

©IJRASET: All Rights are Reserved | SJ Impact Factor 7.538 | ISRA Journal Impact Factor 7.894 |

## III. METHODOLOGY

This chapter sets forth the methodology and work flow followed in this project in brief provides in-depth insights on workflow and research methodology followed in this project




### *A. Methodology Overview*

This study will be focused on reducing the turbo lag of a turbocharger. But before trying to reduce turbo lag we need to know how turbochargers work. Study of existing system is a must for this purpose. we will study the working of a turbocharger and how different types of turbocharger work. The data used in this report has been taken from various online resources.

Selecting a compatible turbocharger is the first step towards solving the problem of turbo lag since bigger turbos will be less responsive than the smaller ones. For this we will learn about how turbines and compressors are selected depending on energy recovery and air flow rate, respectively. Further we will see the analytical data that is used to compare the performance of various types of turbochargers to the performance of a naturally aspirated engine.

*ISSN: 2321-9653; IC Value: 45.98; SJ Impact Factor: 7.538*
*Volume 10 Issue V May 2022- Available at www.ijraset.com*

## IV. DESIGN ANALYSIS OF A TURBOCHARGER

### A. *Types of Turbochargers*

1) *Twin-Scroll Turbo*: Twin-scroll turbochargers need a divided-inlet turbine housing and exhaust manifold to match the right engine cylinders to each scroll. separately. In a four-cylinder engine (with a firing order of 1-3-4-2), cylinders 1 and 4 may feed to one turbo scroll, while cylinders 2 and 3 may feed to another. This configuration allows for more effective exhaust gas energy transfer to the turbo, resulting in denser, purer air entering each cylinder. Again, addressing the complexity of a system needing elaborate turbine housings, exhaust manifolds, and turbos comes at a cost. A schematic of twin-scroll turbo is given below in Fig (4.1).

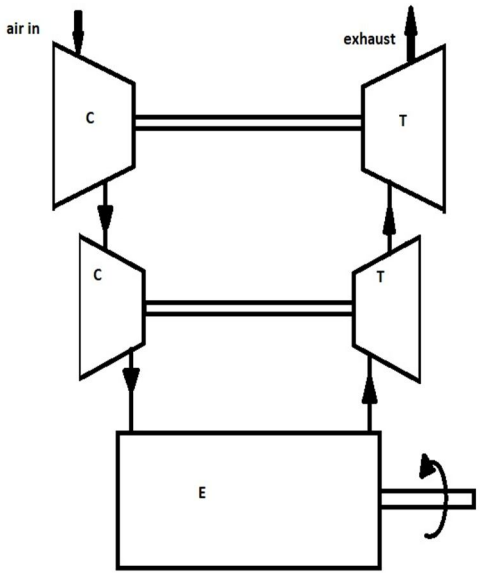



Fig (4.1): Twin-scroll turbo

2) *Sequential Turbo*: When faced with the choice of a small low-end turbo or a big high-end turbo, the solution is simple: fit two, one small and one large. As a consequence, you have a small turbo that comes in early and produces strong torque, as well as a larger turbo that delivers top-end power, resulting in a torque curve that is wide and flat. On the negative side, you're left with an engine that's pricey, heavy, and complicated. A schematic of sequential turbocharger is given below in Fig (4.2).

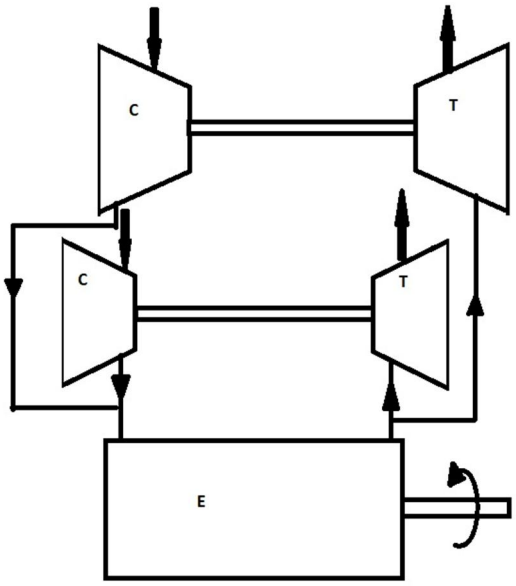



Fig (4.2): Sequential Turbo

©IJRASET: All Rights are Reserved 

3) *Variable Geometry Turbocharger (VGT)*: At the turbine inlet, most VGTs have a ring of aerodynamically formed vanes in the turbine housing. These vanes revolve in turbos for passenger automobiles and light trucks to change the gas swirl angle and cross-sectional area. Internal vanes change the area-to-radius (A/R) ratio of the turbo to match the engine's RPM, resulting in peak performance. A low A/R ratio helps the turbo to spool up fast at low RPM by boosting exhaust gas velocity. The A/R ratio rises with higher rpm, allowing for more ventilation. This results in a low boost threshold, which reduces turbo latency while also allowing for a wide and smooth torque band. While VGTs are more often found in diesel engines with lower-temperature exhaust gases, their usage in petrol engines has been limited due to their high cost and the demand for exotic-material components. The high temperature of the exhaust gases necessitates the use of unique heat-resistant materials for the vanes to avoid damage. As a result, their use has been limited to luxury, high-performance engines. A schematic of VGT is given below in Fig (4.3).

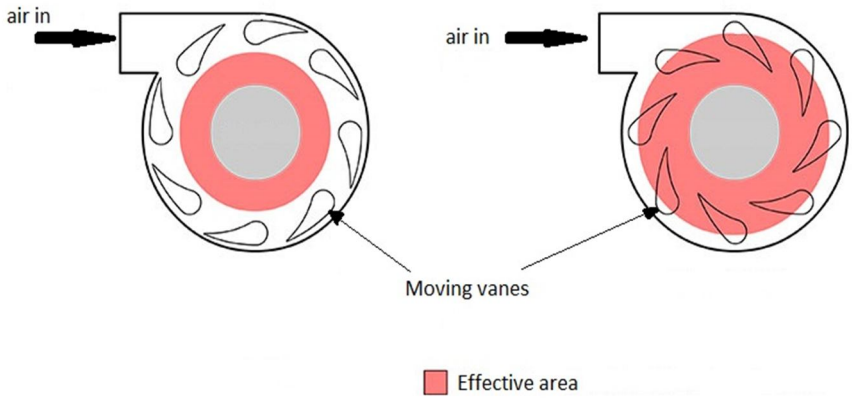



Fig (4.3): Variable Geometry Turbocharger

4) *Electric Turbo*: At lower engine speeds, where a traditional turbo is inefficient, an electric turbocharger is used to decrease turbo lag and aid a conventional turbocharger. This is accomplished by including an electric motor that spins up the turbocharger's compressor from the start and through the lower rpm until the exhaust volume's power is sufficient to operate the turbocharger. The turbine is coupled to a generator and that helps with exhaust gas energy recovery. This method eliminates turbo lag and considerably expands the RPM range in which the turbo may work efficiently, depending on the motor. The majority of the challenges are related to cost and complexity, since the electric motor must be accommodated, charged, and cooled to avoid reliability concerns. A schematic of electric turbocharger is given below in Fig (4.4).

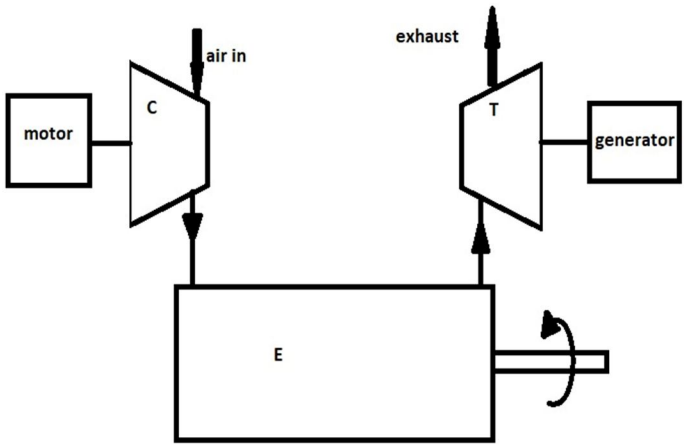



Fig (4.4): Electric Turbo

*B. Types of Turbines*

*1) Constant Pressure Turbine:* The exhaust branch or pipe from each individual cylinder is led into a common manifold in this system. Eddies are set up as the exhaust gas blows into the manifold to help damp out any pressure wave caused by the exhaust gas influx. The manifold's volume must also be large enough to accommodate the gas flow from individual cylinders without causing any localized pressure rise as exhaust gas leaves the cylinder. The effect of enough volume in the manifold in combination with eddies in the exhaust gas from individual cylinders causes the pressure in the manifold to remain nearly constant. At constant pressure, exhaust gas is led from the manifold into the exhaust gas turbocharger. A schematic of constant pressure turbine is given below in Fig (4.5)

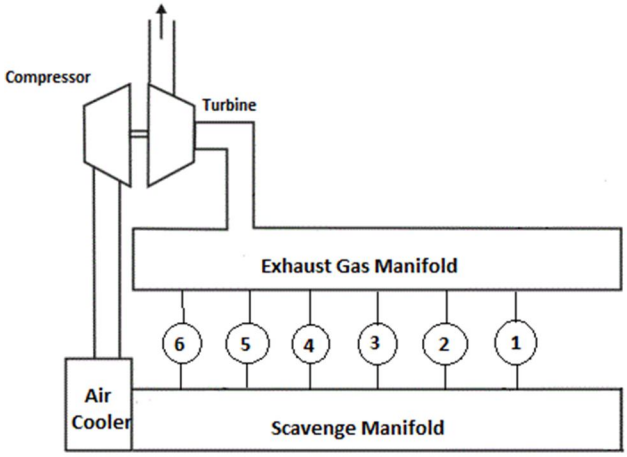



Fig (4.5): Constant pressure turbocharging.

*2) Pulse type Turbine:* In the pulse system, the energy in the exhaust gas is maximized during the blowdown period by designing the exhaust valves with the largest possible port area. The exhaust cams are made to provide the fastest exhaust valve opening possible. The blowdown of exhaust into the exhaust pipe causes a pressure wave or impulse to pass down the exhaust pipe to the nozzle plate in the exhaust turbine when the exhaust valve opens. The exhaust gas static pressure during the impulse period is higher than the air charging pressure, so no cylinder should be exhausting when the impulse passes in the exhaust pipe, or exhaust gas may blow back into the cylinder. Exhaust pipes for engines turbocharged on the impulse system must be carefully grouped in accordance with the engine exhaust valve timing. A separate entry into the exhaust turbine is provided for each group of exhaust pipes, and each entry leads to its own nozzle group. A schematic of pulse type turbocharging is given below in Fig (4.6).

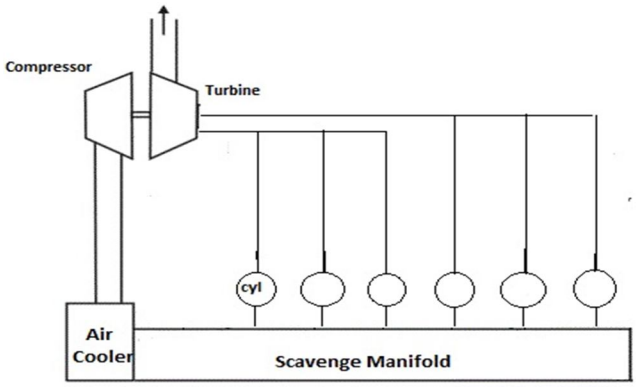



Fig (4.6): Pulse type Turbocharging.

In this chapter we are going to study how we can select a turbocharger for a given engine, and further how can we improve the transient times for the engines. There are several methods explained in this chapter that can be effectively used to reduce the turbo lag, that is the time required for a turbocharger to spool up to the required speed.

*C. Selecting a Turbocharger*

With the Study above we can say that there can be various outputs given by a turbocharger. We will be focusing on the solutions that will help reduce turbo lag. To do that we need a responsive turbine that can generate torque fast enough for those low RPMs. We can see that in sequential turbos and electric turbos. While sequential turbos help reduce the lag, electric turbos eliminate it altogether. We will see what parameters help in the reduction of turbo lag.

Transient time is the time taken by the turbocharger to go from rest to the required state. The A/R ratio of the turbo charger plays an important role in the transient response time of the engine. The Fig (4.) shows how to select the area and radius.

$$\frac{A}{R} = \frac{\text{Area of the passage}}{\text{Radius corresponding to that area}} \quad \ldots. (1)$$

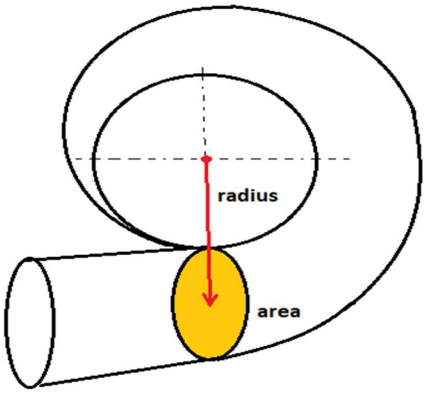



Fig (4.7): A/R of a turbo

The more the A/R of the turbo the more time it will take to reach the required RPM but it will give a much better peak performance compared to a smaller turbo. On the other hand, smaller turbocharger spools up much faster but chokes the engine at higher RPM. To tackle this, we can use sequential turbocharger which is a compounded turbo made of a smaller turbo for responsiveness at lower rpms and a bigger turbo for higher rpms.

For the selection of the compressor part of the turbo, which is the more important part, we have a graph of pressure ratio vs mass flow rate. This is the deciding factor while selecting a compressor for the engine.

Fig (4.8) is performance map of a compressor. The flow limit is represented by the choke line. When a turbocharger is operated far into choke, turbo speeds skyrocket, compressor efficiency plummets (due to extremely high compressor outlet temperatures), and turbo durability suffers. Surge limit line is a line representing the minimum flow below which the compressor will surge (violent air flow oscillating in the axial direction of a compressor). The horizontal lines connecting surge line and choke line are constant speed lines.

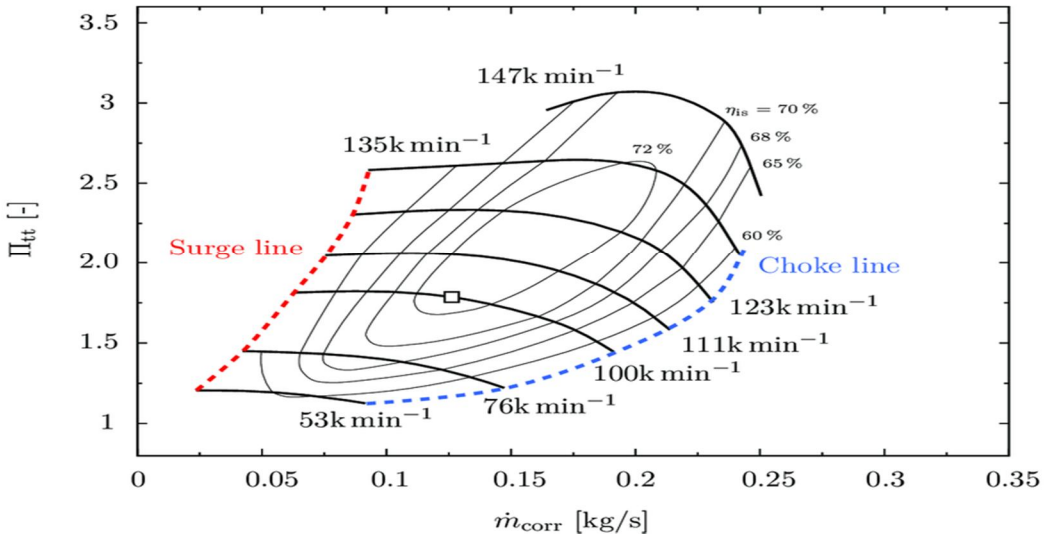



Fig (4.8): Compressor performance map

On the x-axis we have pressure ratio which is given by,

$$PR = \frac{P_{2C}}{P_{1C}} \quad \text{…. (2)}$$

Where,

P2c = Boost Gauge Pressure (PSIg) + Absolute Atmospheric Pressure (PSIa)

P1c = Absolute Atmospheric Pressure (PSIa) – 1 System Depression

and on the y-axis, we have the mass flow rate of the compressor which is given by

$$W_a = \frac{MAP * VE * \frac{N}{2} * V_d}{R * (460 + T_m)} \quad \text{…. (3)}$$

Where,

Wa = Airflow actual (lb/min)

MAP = Manifold Absolute Pressure (psia)

R = Gas Constant = 639.6

Tm = Intake Manifold Temperature (degrees F)

VE = Volumetric Efficiency

| Valves/Cylinders | VE |
|---|---|
| 2 | 0.80 |
| 3 | 0.85 |
| 4 | 0.90 |
| 5 | 0.95 |

Table (4.1) Volumetric Efficiency for given number of cylinders

N = Engine speed (RPM)

Vd = engine displacement in cubic inches

With this information we can plot the data on the performance map and see if the compressor will be efficient for the engine.

*1) Limitations of Experimental Turbocharger Mapping*

*a) Flow Sensor Accuracy:* The flow through the compressor (and the turbine) is typically determined by detecting the differential pressure across a correctly designed orifice in the flow route and using Bernoulli's formula to calculate the flow rate, assuming incompressible flow (constant density). As the flow rate is changed, the compressor characteristics change smoothly. Smaller orifice plates and nozzles can be used to monitor lower flows and map at lower speeds; however, this creates a challenge. The precision of measurements from any one measuring equipment decreases as the flow rate decreases. Changing to a different measuring device suited for lower flow rates at some point creates a step change in the mass flow values when the measurement precision is increased again. This difficulty might be solved by using a large number of orifice plates and nozzles. However, this is not common practice, and improvements rely heavily on the supplier's goodwill.

*b) Heat Transfer Effects:* The heat transfer from the hot lubricating oil to the cold compressor end causes a second difficulty in the low-speed area of the maps. Conduction from the heated air to the lubricating oil might reverse at greater speeds. The heat contributed to the air is monitored by temperature sensors that measure the rise in air temperature and are used to compute the work input and, as a result, the compressor and turbine efficiency. It makes the compressor appear worse since more turbine effort appears to be required than is really used. The similar effect improves the appearance of the turbine. Because of the greater temperature disparities at low speeds, this problem is exacerbated. The backplate and compressor housing are very efficient heat exchangers because they have relatively large surfaces, larger temperature dips, and low flow rates. The compressor maps all show efficiency dropping at low pressure ratios, demonstrating this impact. This isn't real aerodynamic performance. The opposing impact of the turbine seeming better than it is shown on the turbine maps. This is not actual aerodynamic performance, yet again. The heat transfer effect would be more significant at lower speeds. This means that if the maps were utilised without adjustment, the anticipated transient performance would be incorrect since the turbine work to drive the compressor is underestimated and more work is really available to accelerate the rotor. Without separate turbine, bearing, and compressor dynamometers, the heat transfer problem is difficult to solve. When they are used, the compressor mapping method may be tweaked to limit the temperature differences that drive heat transfer, thus eliminating it. Different oil temperatures, on the other hand, may necessitate the use of different bearings, and either of these two modifications would have an impact on the turbine mapping. The turbocharger industry is fully aware of the issue, but easy remedies do not appear to be accessible at this time.

*D. Reducing Turbo Lag*

Because we're interested in what occurs when the throttle re-opens, the graph below shows manifold pressure and throttle position starting halfway through a gearshift.

The manifold pressure trace, in particular, reveals two different zones: initial pressure rise and turbo lag. Graph is shown in Fig (4.9)

The initial pressure increase is similar to that of a normally aspirated engine, in that as the throttle is opened, the manifold pressure rises fast from vacuum to supply pressure (i.e., the pressure upstream of the throttle – on a NA engine, this Is usually atmospheric pressure).

As the manifold equalizes with the supply pressure, the pressure rises at a faster pace, while the turbo continues to spool up. The engine and turbo system dictate the rate of pressure increase during spool up, and the time it takes to do so is known as turbo lag.

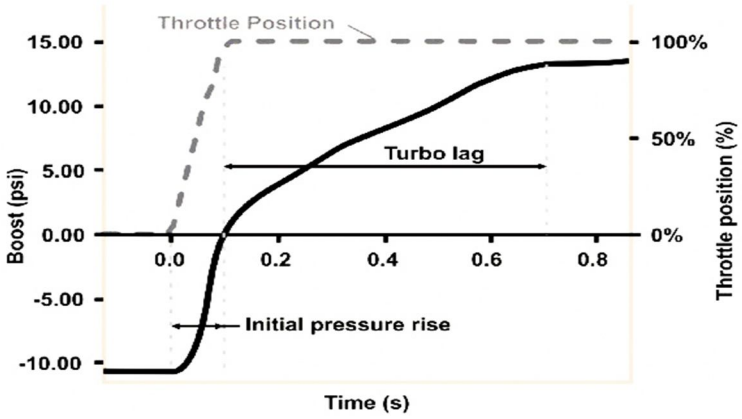



Fig (4.9): response time of a turbo

Several strategies have been proposed to improve the transient response of miniaturized internal combustion engines. This chapter will provide a brief overview of some of the methodologies and related research. Variable geometry turbines, sequential turbochargers and electrical turbochargers are the approaches addressed here.

1) *Variable geometry turbines (VGT):* VGT is a previously stated option that can be actively managed to achieve desirable flow characteristics during a transient. Gravdal et al. [8], demonstrated response improvements in 0-60 mph acceleration times for a 7.3l V8 CI truck in a simulation-based study, as shown in Fig (10). From standstill until the end of first gear, where the turbo-lag effects are most noticeable, a 2-second improvement over a normal turbocharger can be noted.

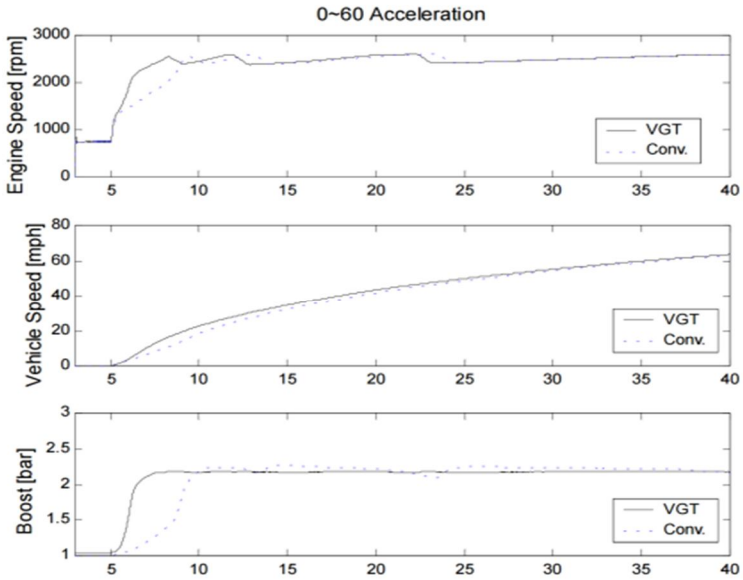



Fig (4.10): VGT vs conventional turbocharged engine

2) *Sequential Turbochargers:* A sequential turbocharger has shared intake and exhaust manifolds. This allows any or both turbochargers to be activated depending on engine speed, significantly increasing the flow range. A transient from low to high engine speed may then use one turbocharger for the first part of the transient and open valves linking the second turbocharger for the second part. The torque development for a 4-cylinder 2.2L CI engine that is fitted with sequential turbocharger and another fitted with a VGT can be seen in the Fig (4.11) below. The benefits of the sequential charging technique can be found to be comparable to those of a 2.7l conventional turbocharged engine.

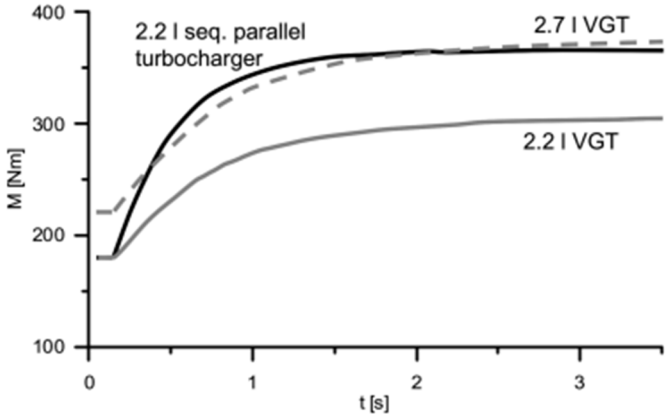



Fig (4.11): A sequential turbocharged engine and a VG turbocharged engine are compared in terms of torque development.

3) *Electric turbochargers:* Electric turbocharger systems have grown in popularity as a result of recent technological advancements in high-speed motor designs, and have been the focus of multiple researches over the last decade. At high speeds and loads, both the use of an electric motor to increase reaction and the use of a generator to capture and store excess exhaust gas energy have been investigated. An electric motor/generator is connected to the turbocharger shaft in an electrically assisted turbocharger. A schematic diagram of the setup is already shown previously. The electric motor supports the turbocharger by accelerating the shaft during transients. By imposing a counteracting torque on the turbocharger while harvesting and storing the energy at the same time, the motor may effectively perform the same task as a VGT or wastegate solution at high loads and speeds. A comprehensive study, led by Gravdal et al. [8], found that using an EATC reduced the time it took to reach the optimum boost level during a load increase by up to 30%. Fig (4.12) shows the transient improvements for a 7.8l inline-6 CI engine. The same study found that alternating between motoring and generating modes reduced fuel usage by up to 5% for driving cycles. In this experiment, an induction motor capable of producing 1 Nm at 60 000 rpm and a continuous power of 6.3 kW at 120 000 rpm was used.

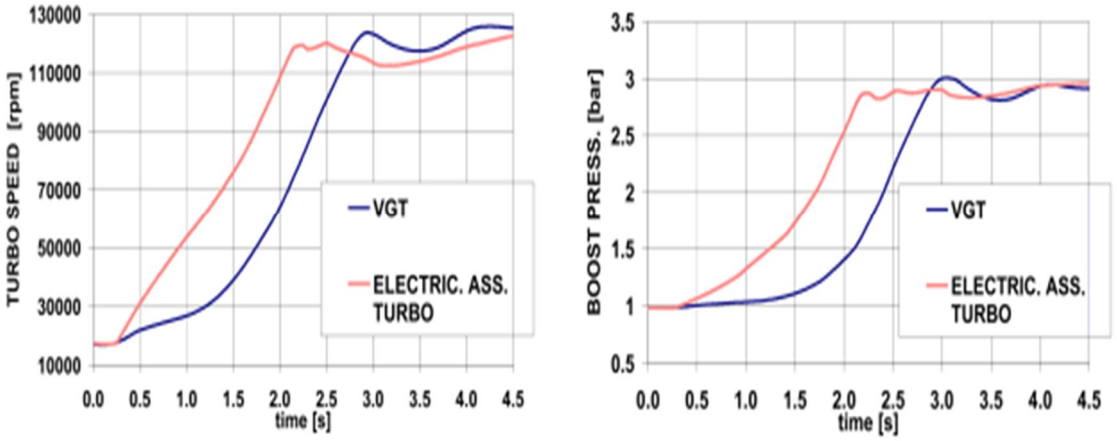



Fig (4.12): Turbocharger speed, and boost pressure response improvements by electrically assisting the turbocharger.

*ISSN: 2321-9653; IC Value: 45.98; SJ Impact Factor: 7.538*
*Volume 10 Issue V May 2022- Available at www.ijraset.com*

## V. SELECTING THE RIGHT TURBOCHARGER FOR A GIVEN ENGINE

For this study we are going to select a turbocharger for the Mercedes Benz M282 Engine, it was first made in 2018 and is being used since. The Engine is built from aluminum. The cylinder block and cylinder head are also made of aluminum, with a spray of plasma coating on the walls that helps in heat conduction and minimizes friction.
Specification:

| | |
|---|---|
| Fuel type | Gasoline |
| Fuel system | Direct Injection |
| Configuration | Inline |
| Number of cylinders | 4 |
| Valves per cylinder | 4 |
| Valvetrain layout | DOHC |
| Bore, mm | 72.2 mm (2.84 in) |
| Stroke, mm | 81.3 mm (3.20 in) |
| Displacement, cc | 1,332 cc (81.3 cu in) |
| Type of internal combustion engine | Four-stroke, turbocharged |
| Compression Ratio | 10.6:1 |
| Power, hp | 109-163 hp (80-120 kW)/5,500 |
| Torque, lb ft | 133-184 lb ft (180-250 Nm)/ 1,375-4,000 |
| Firing order | 1-3-4-2 |

Table (5.1) Specifications of the engine

Now from Fig 4.8 we know that we need PR i.e., the pressure ratio and the $W_a$ which is the actual mass flow rate of the compressor. From (2) we can calculate the PR of this Engine,

$$PR = \frac{\text{Boost Gauge Pressure (PSIg)} + \text{Absolute Atmospheric Pressure (PSIa)}}{\text{Absolute Atmospheric Pressure (PSIa)} - 1 \text{ System Depression}}$$

$$PR = \frac{11.8095+14.7}{14.7-1}$$

So, PR = 1.935

$$W_a = \frac{MAP * VE * \frac{N}{2} * V_d}{R * (460 + T_m)}$$

For this engine,
MAP = 28.44
VE = 0.9
N = 6000 (upper limit for calculation)
Vd = 81.3
R = 639.6
Tm = 140
Substituting these values in the formula we get,

$$W_a = \frac{28.44[0.9 * (\frac{6000}{2}) * 81.3]}{2639.6(460+140)}$$

$$W_a = \frac{6242864.4}{383760}$$

$W_a$ = 16.29 ≈ 16.3 lb/min
$W_a$ = 0.123 Kg/s
We got,

PR = 1.935
$W_a$ = 16.3 lb/s or 0.123 Kg/s
After going through a lot of compressor-maps we found the Garrett GBC17-250 to be the most suitable one for our selected engine. The compressor map of GBC17-250 with the selected engine parameters marked on the graph can be seen below in the Fig (5.1) taken from [13].

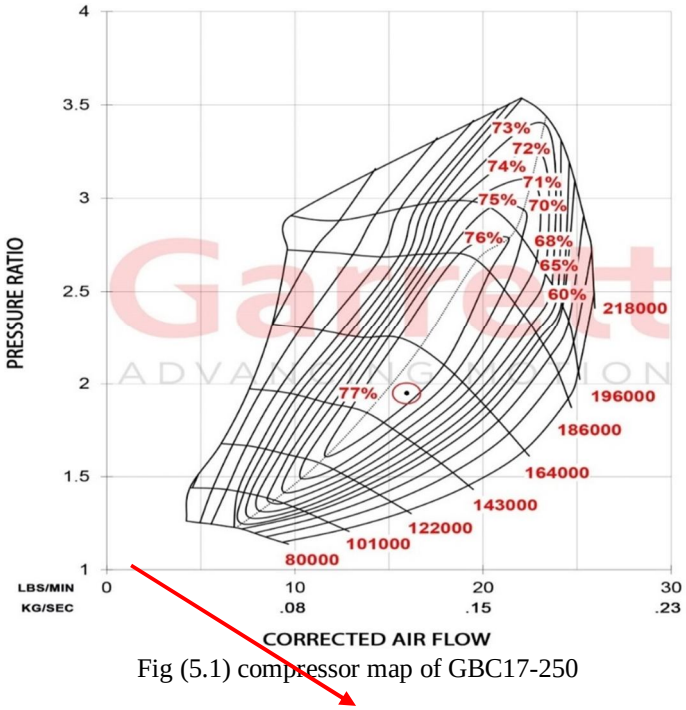



Fig (5.1) compressor map of GBC17-250

It lands on the most efficient contour and so we can say that this model of Garrett is best suited model for this engine

An image of the selected model can be seen below in Fig (5.2)




Fig (5.2) GBC17-250 product image

Other specifications of this model are given below

| Compressor | | | | Turbine | | | | | |
|---|---|---|---|---|---|---|---|---|---|
| Inducer | Exducer | Trim | A/R | Inducer | Exducer | Trim | A/R | Inlet | Outlet |
| 36mm | 49mm | 55 | 0.52 | 44mm | 40mm | 80 | 0.50 | T25 | 5 Bolt |

Inducers are the intake fan of the turbine and Exducers are the outlet fans of the turbine as seen in the Fig (5.3) below

Trim = $\left(\frac{Inducer^2}{Exducer^2}\right) * 100$

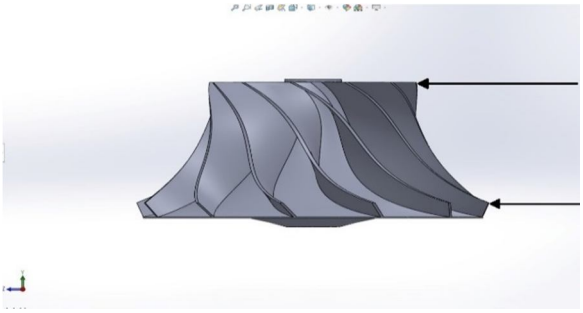



Fig (5.3) Inducer and Exducer

## VI. MATERIALS THAT CAN BE USED FOR TURBINE NOZZLE

Because diesel engines have a lower exhaust temperature (compared to petroleum - based engines), the technology has been successfully utilized in diesel engines for the past 20 years, allowing for the use of low-cost materials. Due to high exhaust gas temperatures, this is not the case for gasoline engines. In light of this technical obstacle, the current study examines attempts to use VGTs in petrol engines and analyses other material possibilities that would be suitable for use in a VGT's adjustable nozzle portion. A typical VGT's working environment includes exhaust gas temperatures of up to 1050°C and working pressures exceeding 2 bar.

### *A. Candidates for material*

Determining and selecting the class of materials that can be picked as a suitable candidate was made easier by defining the expected degree of performance from the material.

Technical ceramics like silicon carbides and nitrides were chosen because they have great strength at 1000°C. High-grade stainless steels, which were also acceptable candidates for the application, can derive the same conclusion. The performance of critical mechanical qualities in a turbocharged setting was compared using a super alloy, IN 751, which is ideal for such applications. With Nickel, Cobalt, or Nickel Iron as the basis alloying element, super alloys and high temperature alloys display outstanding mechanical strength, creep resistance, corrosion and oxidation resistance, and surface stability at high temperatures. These alloys can only be used in high-end turbomachinery applications, thus their usage in mass-produced automobiles is not justifiable. For this reason, compounds that are used in automotive systems could be evaluated to see if they meet the requirements for VGT application. Exhaust valves, the exhaust plenum, and the turbocharger turbine are among the components of the exhaust system that have been examined for the cloth selection process and may be exposed to high exhaust gas temperatures (and pressures). The additives' own resistance to oxidation and corrosion when exposed to high temperatures. The most recent trends in the development of oxide scales in high-temperature conditions make them suitable candidates for use in VGT nozzle systems. Materials used in various turbocharger components, such as turbine wheels, turbine housings, and the waste-gate valve, were also considered in order to provide reliable data. Inconel is often used to make turbine wheels. These alloys could be utilized in mass-produced autos, but Mitsubishi Heavy Industries Limited is developing a new fabric dubbed MarM for high-performance engines (MHI). The material is difficult to cast and may contain minor casting flaws. To avoid this, MHI uses a process called Hot Isostatic Pressing (HIP), which gives the material a uniform structure. The creep rupture of a turbine wheel when utilized at 1000°C and circled at extremely high speeds is depicted in Fig. 2. On the rear fringe of the turbine, the rupture begins near the roots of the blades. Furthermore, tests comparing the MarM material to Inconel demonstrate that the MarM material has nearly three times the creep life of Inconel.

©IJRASET: All Rights are Reserved 

1) *Carbides of Titanium Silicon :*A turbine's blades must withstand high temperatures for long periods of time, making it the most difficult engineering product ever created. This scenario might also apply to the aerofoil-shaped vanes. Materials used in this section are usually known as MAX phase elements They are made up of early transition metals "M" (red) from the periodic table's "A" group (blue), commonly IIIA and IVA, and a substance "X" that contains either nitrogen or carbon. The source of origin of the MAX phase metals on the periodic table is depicted in Fig (6.1). Ternary ceramics are a type of ceramic that was found in the early 1960s. The material can withstand temperatures up to 1400°C and decomposes at a temperature of 2000°C.

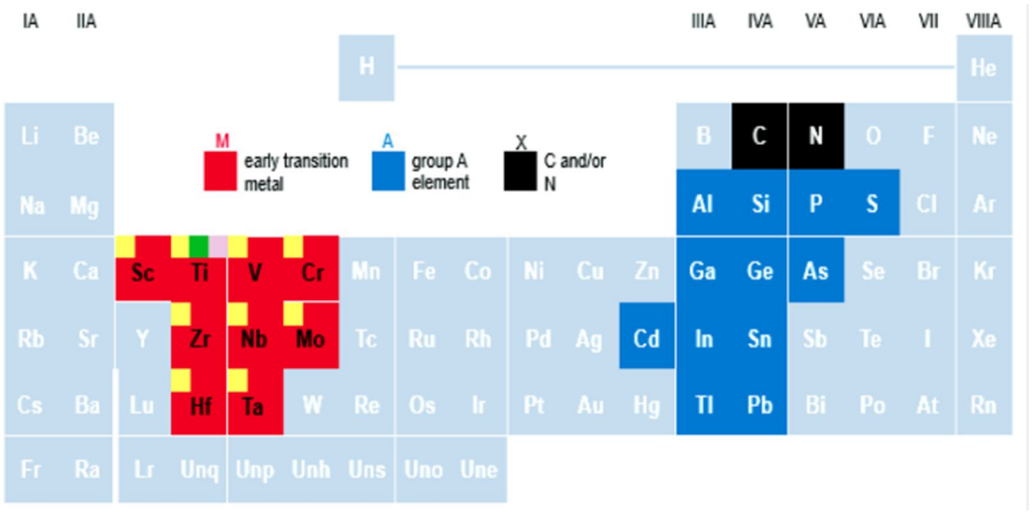



Fig (6.1) Materials for “M” and “A” phases in MAX phase elements

Under stress and at high temperatures, the materials on the right have superior rupture resistance. Higher oxidation resistance is seen in the materials near the top of the picture. Dislocation faults arise at roughly 1200°C, causing deformation of more than 20% in tension, compression, and bending. The ternary material has a particular advantage over other ceramics because of its loadbearing capacity even after deformation. These materials' highly oriented grains give the requisite strength and capacity to operate as a ductile material, lowering the factor of safety needed to build machines that are subjected to high temperatures.

Pesyridis et al. [9] conducted investigations to assess the compression response of Ti3SiC2 at 50-120 GPa, as well as a shock loading pressure of 22–58 GPa and a shock loading temperature of 3250°C, and no symptoms of rupture were discovered in the compound samples.

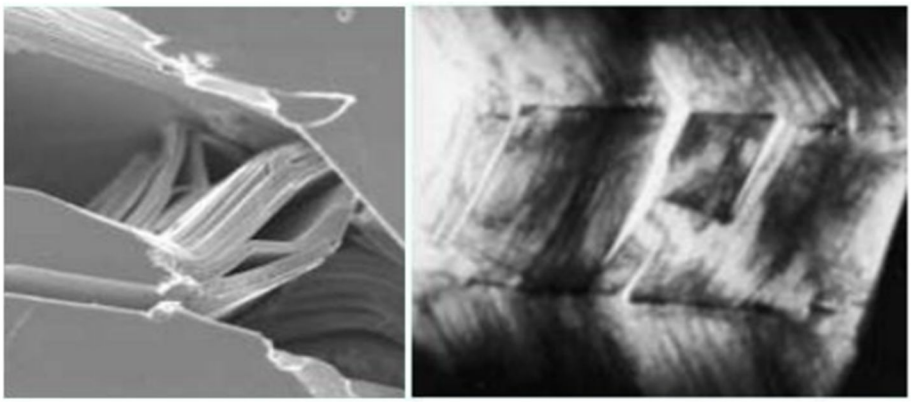


Fig (6.2) Fracture sample of Ti3SiC2 observed under optical and electron (right) microscope

The severe shear stiffness demonstrated is more than five times that of an isotropic material. The ceramic now costs £26 per kg, which is comparable to titanium powders. These materials are inexpensive to produce and may be processed using Pulse Discharge Sintering techniques. Nearly single phase Ti3SiC2 was discovered to demonstrate plastic deformation at ambient temperature, indicating good machineability.

©IJRASET: All Rights are Reserved | SJ Impact Factor 7.538 | ISRA Journal Impact Factor 7.894 |

*2) Stainless Steel 353MA:* As indicated in Fig (6.2) [9], turbocharger housings are typically manufactured of ductile cast iron for temperatures up to 700°C and austenitic stainless cast steel for temperatures up to 1050°C.

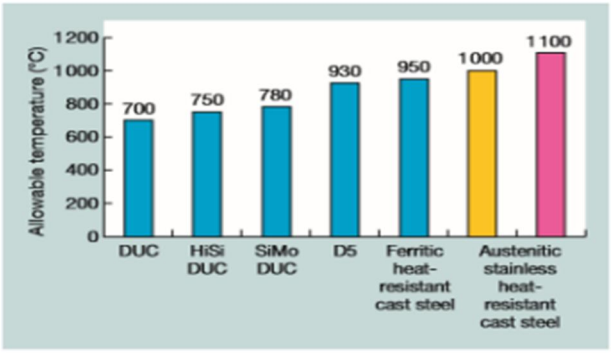



Fig (6.3) Turbine housing material and allowable temperature

Due to the presence of a small quantity of nickel improves creep power and resistance to oxide spallation because of fluctuations in temperature as a result growing resistance to corrosion. Carbon and nitrogen additionally growth the creep power via way of means of forming chromium carbides and nitrides at intermediate temperatures. This material consists of nitrogen, silicon and uncommon earth metals which additionally consists of Cerium. Cerium in aggregate with silicon improves oxidation resistance, erosion and corrosion resistance. To withstand excessive temperature corrosion, nitrogen delays the precipitation of sigma phase. The creep power of SS 353MA for 100,000hours in assessment done by Pesyridis et al. [9] with different austenitic grades may be visible in under Fig (6.3). Reference Steel SS 253MA. Because of the presence of a tiny amount of nickel, creep power and resilience to oxide spallation due to temperature changes improves, resulting in increased corrosion resistance. At intermediate temperatures, carbon and nitrogen also increase creep power by generating chromium carbides and nitrides. This fabric contains nitrogen, silicon, and rare earth metals, as well as Cerium. Cerium improves oxidation, erosion, and corrosion resistance when combined with silicon. Nitrogen retards the formation of the sigma phase in order to endure high temperatures. Fig (6.3) shows the creep strength of SS 353MA after 100,000 hours of testing with various austenitic grades. SS 253MA is a reference steel.

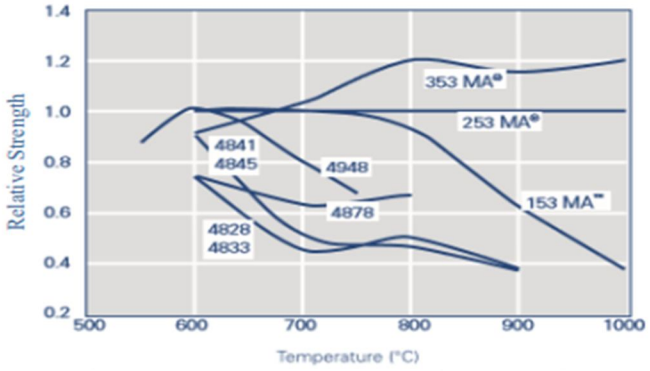



Fig (6.4) Relative creep strength for rupture in different stainless steel

At 900°C, other steel grades are just half as strong, needing double the thickness for the same component. As a result, 353 MA is a good contender for a VGT turbocharger's vane and vane ring assembly. In many applications, SS 353MA has outperformed Inconel alloys due of its superior thermal stability. Because SS 353MA is a ductile metallic material, yield stress can be regarded as destructive stress.

*3) Inconel:* IN 751 are commonly found in hot exhaust from internal combustion engines, where they are mostly employed for exhaust valves. Nickel-based superalloys were chosen as the most suitable material category for operation at high temperatures. Within this class, yield stress, creep, thermal expansion, oxidation, and cost were examined between IN 600, IN X750/751, MA754, and CMSX-4. IN X750 or IN 751 was deemed to be the best suited material for yet another variable geometry application after a qualitative assessment and using the weighted property index approach.

*B. Simulation*

With suitable materials having been identified the next step then involved collecting appropriate engine and turbocharger data for the modeling of the turbine for the purposes of CFD. The following essential steps were taken:

The first step involves accumulating flow parameters such as exhaust gas pressure, velocity and power generated at three different stages i.e., at low, partial and high loads. In second stage the above-described parameters will be used as input for CFD analysis for vanes which will be positioned at three different angles replicating practical situation. This will characterize surrounding fluid flow resulting pressure and temperature on the vane surface. Structural analysis will be performed on the basis of the obtained fluid flow characteristics. This data can then be compared to one of the existing materials used in high end applications which will be a benchmark for evaluating the selected materials. This information can then be matched to other existing high-end materials, which will serve as a baseline for evaluating the chosen materials.

An inline four-cylinder 1.3L SI engine was chosen for study. This engine belongs to the mass-produced passenger SI engine category; however, it provides a demanding turbine environment.

The data for constraints utilised in CFD analysis are listed in Table (6.1) below

| Vane angle (deg) | Average velocity of exhaust gas (m/s) | Absolute Pressure (Bar) | Heat generated ($kW/m^3$) |
|---|---|---|---|
| 70 – closed | 70 | 0.96 | 17143 |
| 55 – mean | 70 | 1.07 | 48571 |
| 40 – open | 70 | 1.09 | 24286 |

Table (6.1) Data constraints for CFD

The power produced by the engine during 3 stages of operation is the value of heat created obtained from the simulation. The greater value was used to evaluate the functionality of the vanes in harsh conditions. The turbine shape and vane assembly were initially developed in Catia. After conducting studies on the construction of VGT vanes, a Catia model was created. In agreement with turbocharged diesel engines in this size category, 9 vanes were chosen.

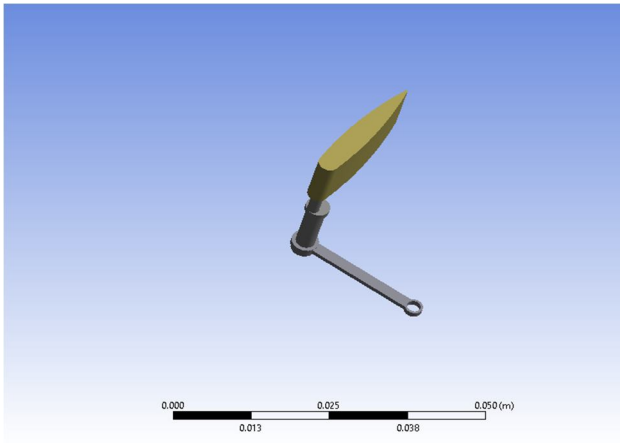



Fig (6.5) Single Vane assembly

The vane is linked to a cylindrical support that acts as a pivoting mechanism, as shown in Fig (6.3). The support's upper circular section is attached to an actuating ring, which is driven by an external actuator. The vane assembly is shown within the housing.

In Ansys Design Modeler, similar vanes were constructed and imported. The length of the vanes was measured in several design iterations. The interspace distance between the vane trailing edge and the rotor inlet had to be set correctly because this essential geometric element influenced flow separation and reattachment. The assembly can be seen in Fig (6.4) below

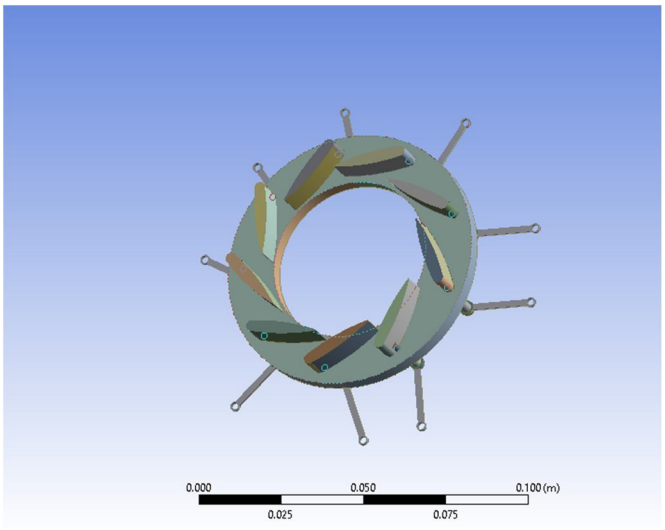



Fig (6.6) Vane full assembly

The inputs for the CFD analysis of vanes are detailed in Table (6.2)

| | |
|---|---|
| Inlet Temperature (K) | 1323 |
| Average turbine inlet velocity (m/s) | 70 |
| Absolute turbine Inlet Pressure (bar) | 2 |
| Number of Iterations | 300 |

Table (6.2) inputs for the CFD analysis of vanes

After the flow analysis, the structural analysis was performed, which included the impacts of temperature and pressure on the vanes. When the several modules of Ansys 2022 R2 are linked together, the programme transfers these impacts with in form of results. In the following section, the imported temperature and pressure loads will be applied and assessed. The solver in the structural analysis module requires a mesh to be constructed for the load-bearing component. The mesh that was constructed is shown in Fig (6.5).

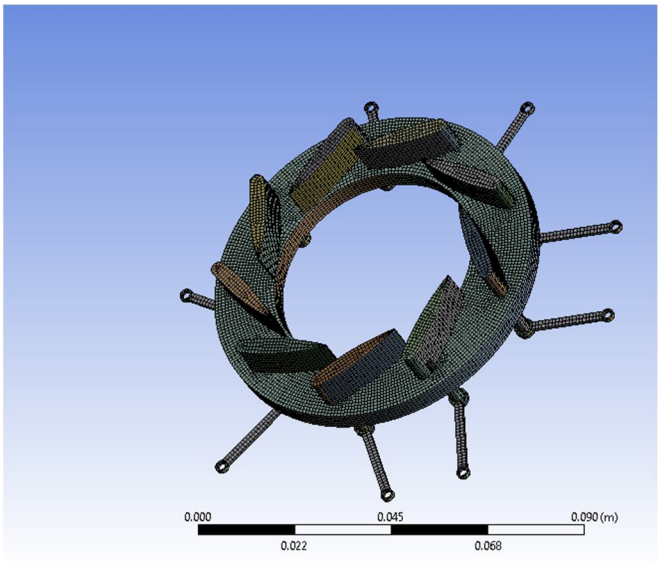



Fig (6.7) meshing completed on vane assembly

During the structural simulation, a moderate triangular mesh was created and optimised. The quality of the mesh was maintained throughout the study in order to compare the extent of distortion of the selected three materials and to ensure computational consistency. Once the throat area expands to offer optimal airflow with in open position, the flow direction is normal distributed towards the vane surface. This could be the main cause of air accumulating at the vane's leading edge, resulting in localised high-pressure zones that generate torque at the hinge. There are two advantages to using VGT at fast engine rpm. It has a higher efficiency because the rear tip of blade is nearest to the turbine wheel, allowing each vane to direct the most quantity of exhaust gas with the least degree of flow separation. This lowers the incidence variation, which is relatively substantial in a fixed shape turbocharger due to viscous effects. The radius where the vanes are situated affects the turbine's efficiency. The best turbine efficiency is likewise found for totally open vanes when the pivoting points are situated as close to the middle of the turbine shaft as feasible. As a result, a compact turbocharger turbine can function at better efficiency at higher engine speeds.

It was necessary to determine on mechanical environment that VGT vane will encounter during the assembly's lifetime in service before completing FEA analysis. The combined combination of the exhaust gases' pressure and warmth would cause the vane to distort. Externally, the linkage is maintained by an actuator that serves like a pivot point for system while also maintaining the vane angle in relation to engine speed.

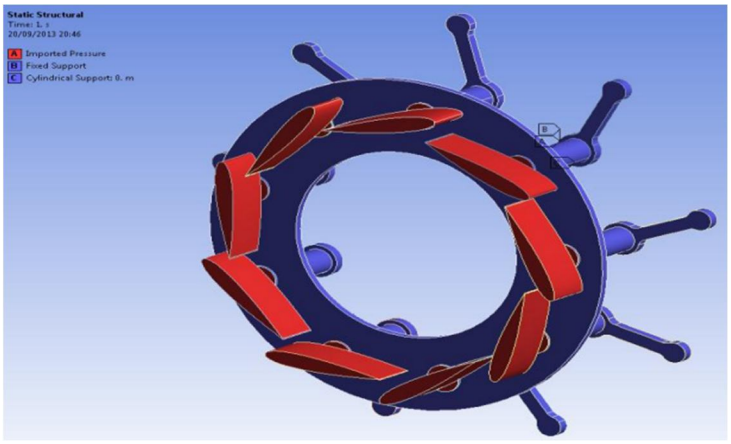



Fig (6.8) Fixed and moving parts

The pivoting shaft was categorized as cylindrical assistance for the study, and the links were categorized as fixed support, as shown in Fig (6.6). On the vane surface, imported pressure was induced. This can simulate the real-world situation in which the links serve as a support framework for rotating the vanes to the desired angle. The temperature and pressure charts are shown in Fig (6.7) and (6.8) below.

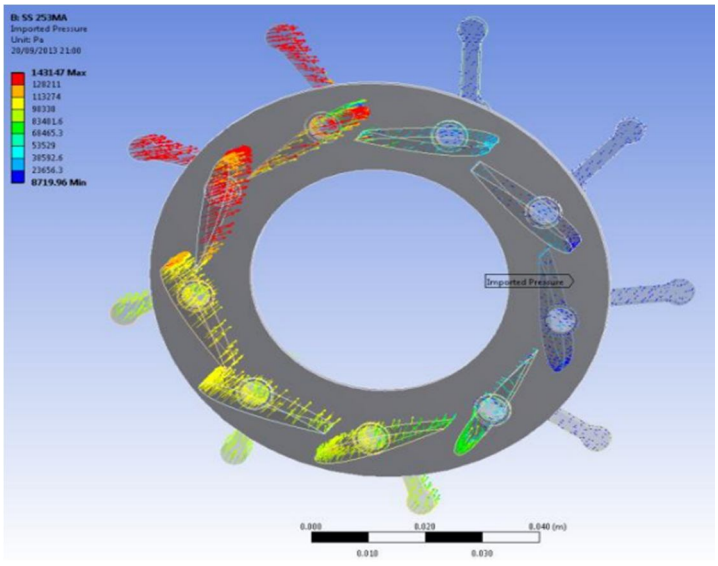



Fig (6.9) pressure variation on the assembly

This pressure acting on vanes is greatest on the left, as seen in Fig (6.7). This is due to the turbine's volute profile, which has the strongest pressure at the beginning and gradually decreases even as area is constrained.

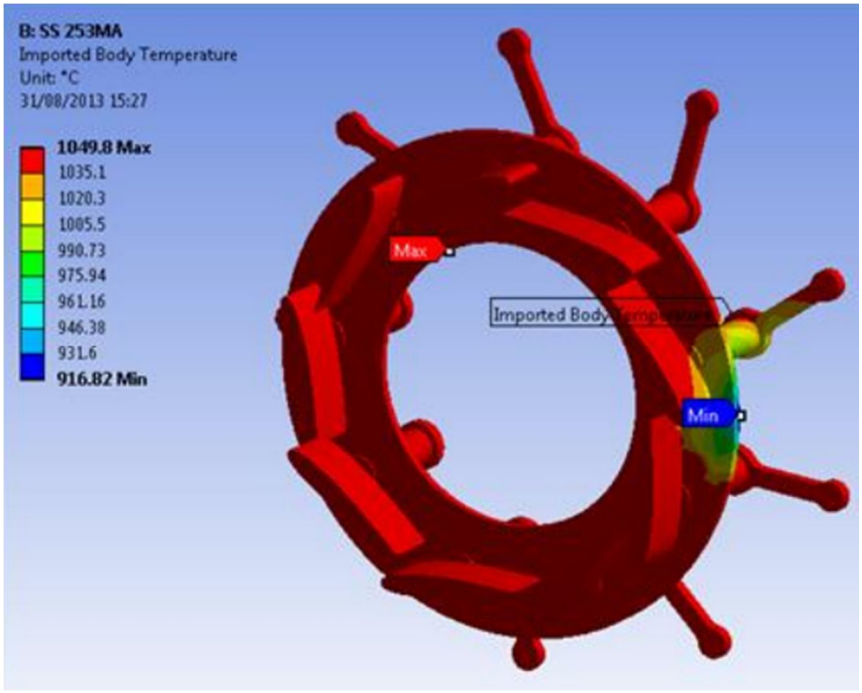



Fig (6.10) temperature contours on VGT assembly

The temperature of engine exhaust has a negative impact on the vane rings and connection, as shown in Fig (6.8). A few inconsistencies were discovered when importing the pressure plots, with the maximum pressure impacting on the vane being higher than in the imported pressure graphs. A direct solver has been used to improve the accuracy. Because the direct solver relies on unidirectional input variables from the user, the results must be carefully validated. The vanes were also subjected to several design iterations in order to improve their structural qualities. The position of the pivot on the vane area was also taken into account. The outer part of the vanes has a cantilever effect due to the exhaust gas flow applying tensions. As a result, the pivot point's distance from the top edge was iterated until the best position was found. By placing the pivot at 1/3rd of the overall length, the distortion was kept to a bare minimum. The similar stresses, equivalent strains, and deformation measured in the three materials will be presented in the following section. Table 7 shows the magnitude of the stresses operating on the vane:

| Material | Yield Stress (MPa) |
|---|---|
| IN 751 | 111.09 |
| Ti3SiC2 | 105.57 |
| SS353MA | 774.1E+02 |

Table (6.3) Yeild stress for different materials

In compared to IN 751 and Ti3SiC2, SS 353 MA appears to be subjected to more stress.
The inventors have also deposited a chromium layer, which provides the materials with oxidation resistant capacity at temperatures greater than 1400°C, using a patented procedure.
Table 8 shows the overall deformation that was recorded:

| Material | Total Deformation (mm) |
|---|---|
| IN 751 | 4.2E-02 |
| Ti3SiC2 | 2.9E-02 |
| SS353MA | 0.24 |

Table (6.4) Total Deformation for different materials

The highest elastic strain for SS 353MA is 0.04 as shown in table 9, while the strain encountered by IN 751 and Ti3SiC2 is 6.17E-05 and 4.54E-05, respectively. The area between both the leading and trailing edges of all three materials shows the most strain. This can be explained by the force exerted on the surface as well as the reaction of the vanes' permanent support.

| Material | Elastic Strain (m/m) |
|---|---|
| IN 751 | 6.17E-05 |
| Ti3SiC2 | 4.54E-05 |
| SS353MA | 0.04 |

Table (6.5) Elastic Strain for different materials

## VII. TRANSIENT OPERATION FUNDAMENTALS:

Transient operation is defined by rapid changes in operating conditions, which can be especially demanding in terms of engine response and the reliability of fuel pumps and governors/controllers, necessitating proper interconnection between the engine, governor, fuel pump, turbocharger, and load via an appropriate control strategy. To avoid over- or under-speeding, overshoot of exhaust emissions, or (substantial) divergence from acceptable fuel consumption limits, the latter is essential.

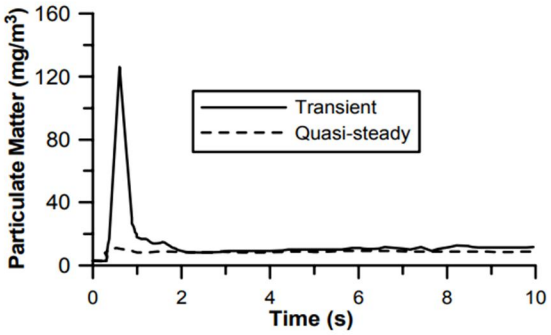



Fig (7.1): Transient vs. steady-state PM emissions during a typical load increase event of a turbocharged diesel engine.

### *A. Typical Transient Operation Cases*

There are a range of 'transient' operating circumstances that engines encounter; they can last anywhere from a few seconds to many minutes. We are considering two forced changes in load and/or fueling:

#### *1) Load Increase (Acceptance) Transient Event*

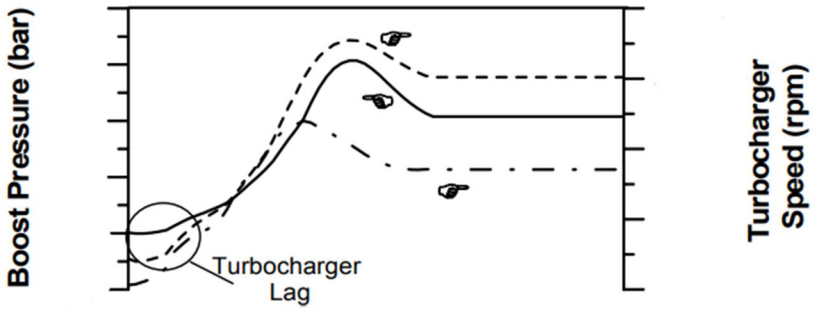



Fig (7.2) Development of engine and turbocharger properties during a load increase transient event.

At the initial conditions, the engine and load (resistance) torque are equal at the start, and the air–fuel ratio is comparatively high. Because the engine torque cannot quickly meet its increased load counterpart, there is a considerable shortfall in the net (engine minus load) torque as soon as the new higher load is applied. As a result, the engine speed lowers. Because the air supply cannot immediately meet the greater fueling due to the turbocharger's delayed response in generating up the requisite delivery pressure, the air–fuel ratio declines. As a result, the instantaneous relative air–fuel ratio may fall below stoichiometric levels, resulting in unpleasant smoke emissions. At the same time, the higher gas temperatures caused by low air–fuel ratios result in higher NOx emissions, with the amount of available oxygen playing an important role.

©IJRASET: All Rights are Reserved 

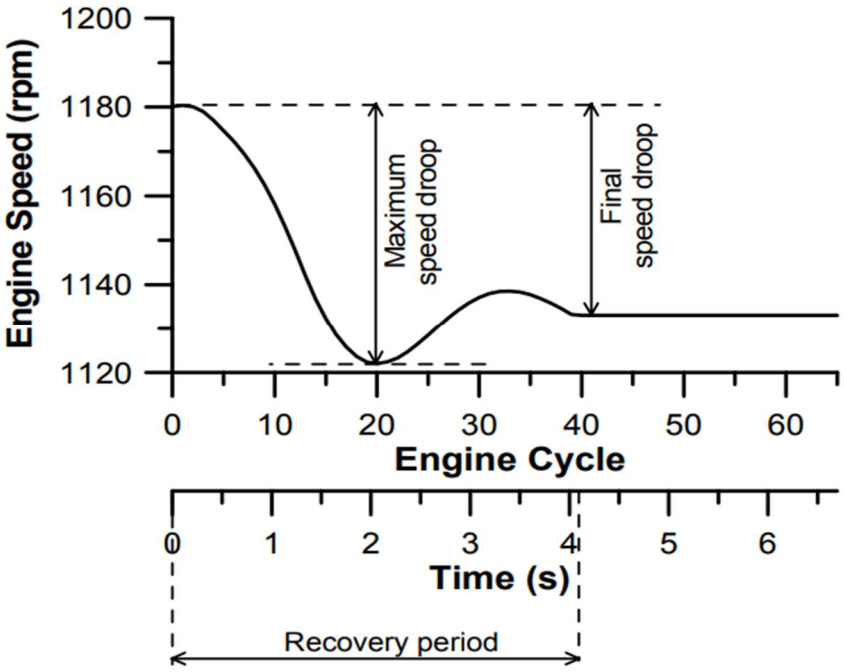



Fig (7.3) Maximum and final speed drop and recovery period for a load acceptance transient event

2) *Speed Increase (Acceleration) Transient Event:* The governor reaches almost instantly its maximum fueling position, remaining there for most of the transient event; the fuel limiting function determining the exact fueling response at the early cycles where the greatest crankshaft acceleration (or deceleration) is established due to the elevated surplus or deficit of torque, respectively; crankshaft acceleration (or deceleration) is established owing to the high surplus or deficit of torque; crankshaft acceleration (or deceleration) is established owing to the high surplus or deficit of Both transients have side effects such as turbocharger lag or exhaust emissions overshoot, with the acceleration transient being heavily impacted by the initial engine loading.

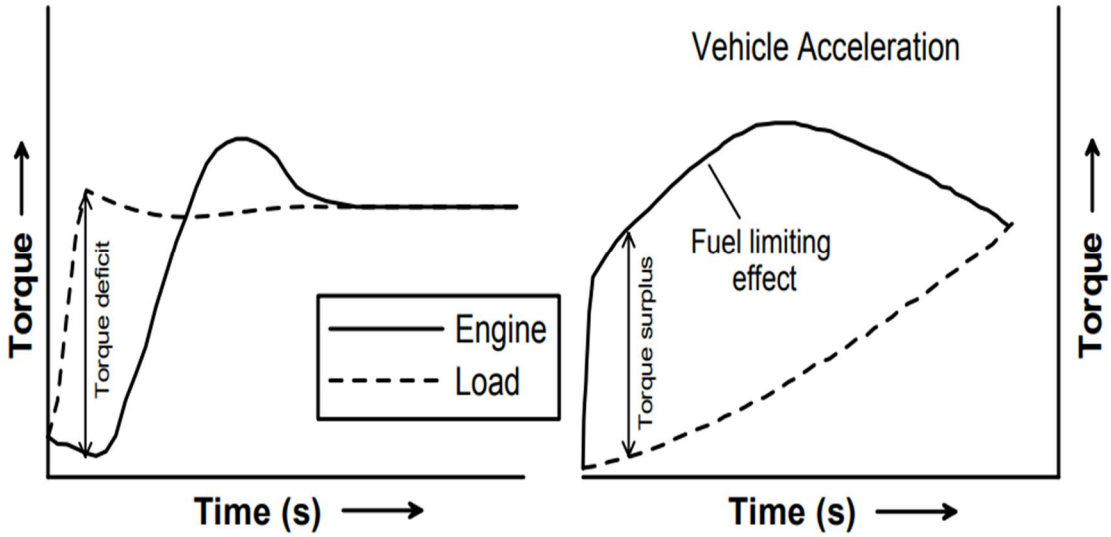



Fig (7.4) Comparison of torque development between typical load acceptance and acceleration transient events.

Despite the lesser magnitude of turbocharger lag effects compared to a severe load acceptance example, substantial levels of smoke emissions are seen during the early cycles of acceleration due to the initially low air–fuel ratio, since fueling has increased considerably faster than air supply.

*ISSN: 2321-9653; IC Value: 45.98; SJ Impact Factor: 7.538*
*Volume 10 Issue V May 2022- Available at www.ijraset.com*

## VIII. MATERIALS

### *A. Electrical generator*

The electrical generator's nominal speed is 10,000 rpm, however we employed an overstressed mode for the electrical generator at 16,000 rpm for a brief period of time (0-20 s)




- Motor Type: XD3420.
- Low Noise Type: < 30dB.
- Operating Voltage: 6~20Vdc. (Nominal 12Vdc)
- No Load Speed: 3,500 RPM @ 12V.
- Rated current: 400mA @ 12V.
- Rated Torque: 19.6N.cm/2Kg.cm.
- Long Life: 3,000 Hours Continuous operation.
- Replaceable Carbon Brush.
- Overall Size: 97 x Ø51 mm.
- Shaft: Full Round Type Ø8mm.
- Weight: 500g.

.

Fig (8.1): XD3420 Electrical generator.

Depending on the values of pressure and compressed air flow in the turbine blades, the electric generator (XD-3420) may create energies of 0.67–0.68 Wh in approximately 21s of the proven testing phase.

### *B. Gear Box*

As we need larger gear ratio to increase the output torque through the motor, we have selected PLM120 Neugart as a gear box for driving the turbocharger shaft. PLM120 Neugart is a Planetary Gear. Because of its low-friction bearing design and optimal lubrication, it is particularly light, incredibly powerful, and yet appropriate for complicated manufacturing cycles. Selected gear ratio is 1:10.



- Frame size: 120
- Nominal output torque: 5-800Nm
- Radial Force: 200-5000N
- Axial force: 200-5000N
- Torsional backlash: 6-22 arcmin

Fig (8.2) PLM120 Neugart.

©IJRASET: All Rights are Reserved 

## IX. SIMULATION USING AMESIM SOFTWARE:

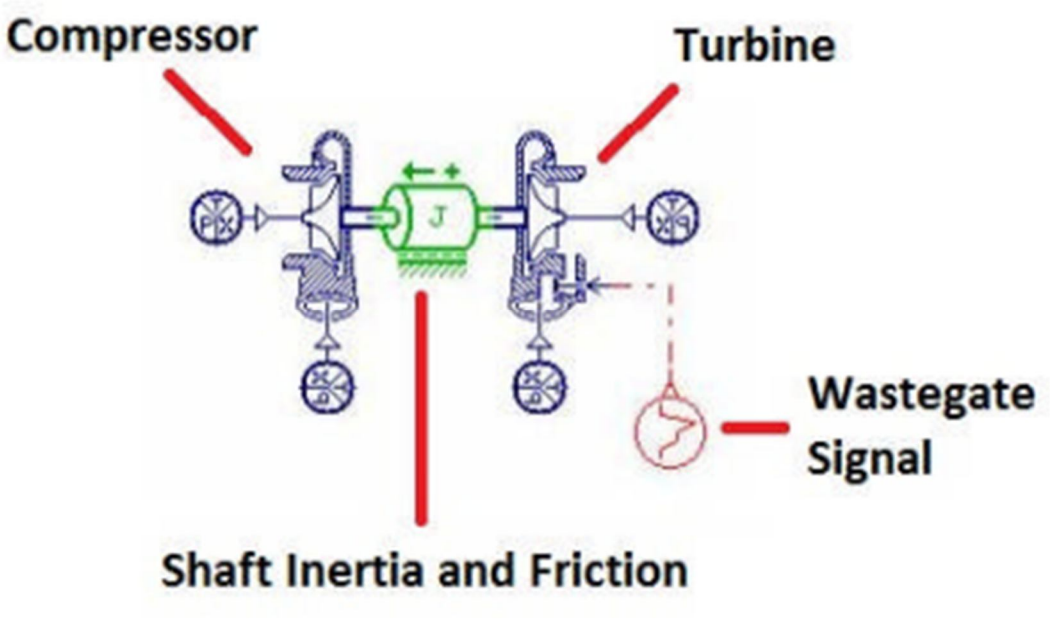
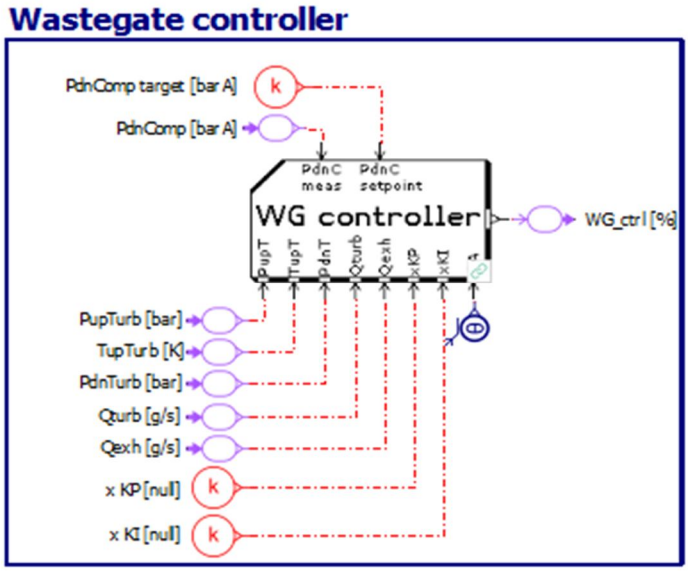



Fig (9.1): AMESIM turbocharger model

There are three ports on both the compressor and turbine types, two pneumatic and one mechanical. The compressor and turbine's pneumatic ports are linked to the intake, exhaust, and atmospheric pressure, respectively. Energy converted from exhaust fumes is transmitted from the turbine to the compressor via the mechanical port. Look-up tables from test data are used to simulate the turbine and compressor. The pressure ratio and efficiency as a function of mass flow rate and rotating velocity are necessary for the compressor. The mass flow rate and enthalpy flow rate may be estimated using the torque applied to the shaft and the efficiency maps. Additionally, the compressor's operation is limited by both choke and surge limitations.

Similarly, the turbine is represented using two types of lookup tables: mass flow rate and efficiency as a function of pressure ratio and rotational velocity. Back-flow and waste-gating are also taken into consideration in this model. Orifices are used to mimic both, with the wastegate controlled by an external command. The wastegate controller is further divided into;

Model Based feed forward, PI controller feedback and Reversed wastegate control law.



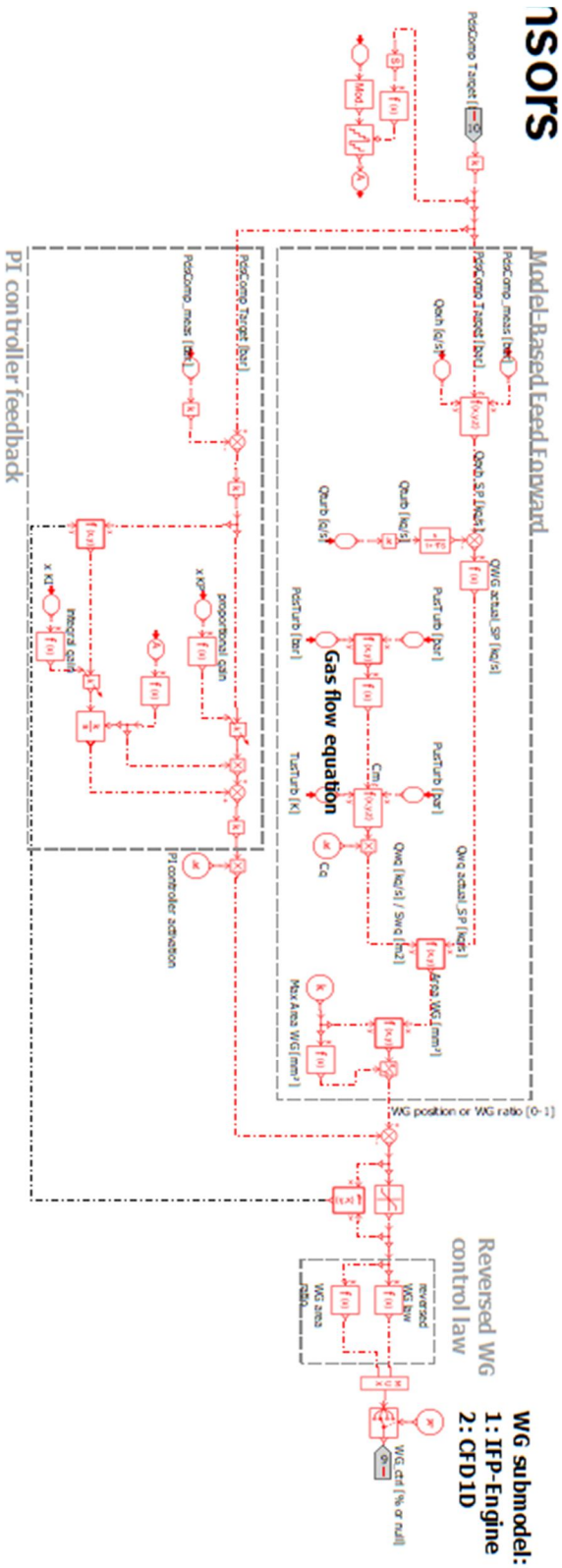



Fig (9.2): Wastegate controller sub model.

As like the wastegate controller sub model, throttle control sub model is made. It basically transmits the signal of throttle input to the system when needed. The model is distributed in three different stages;

Model Based feed forward, PI controller feedback and Reversed throttle control law.

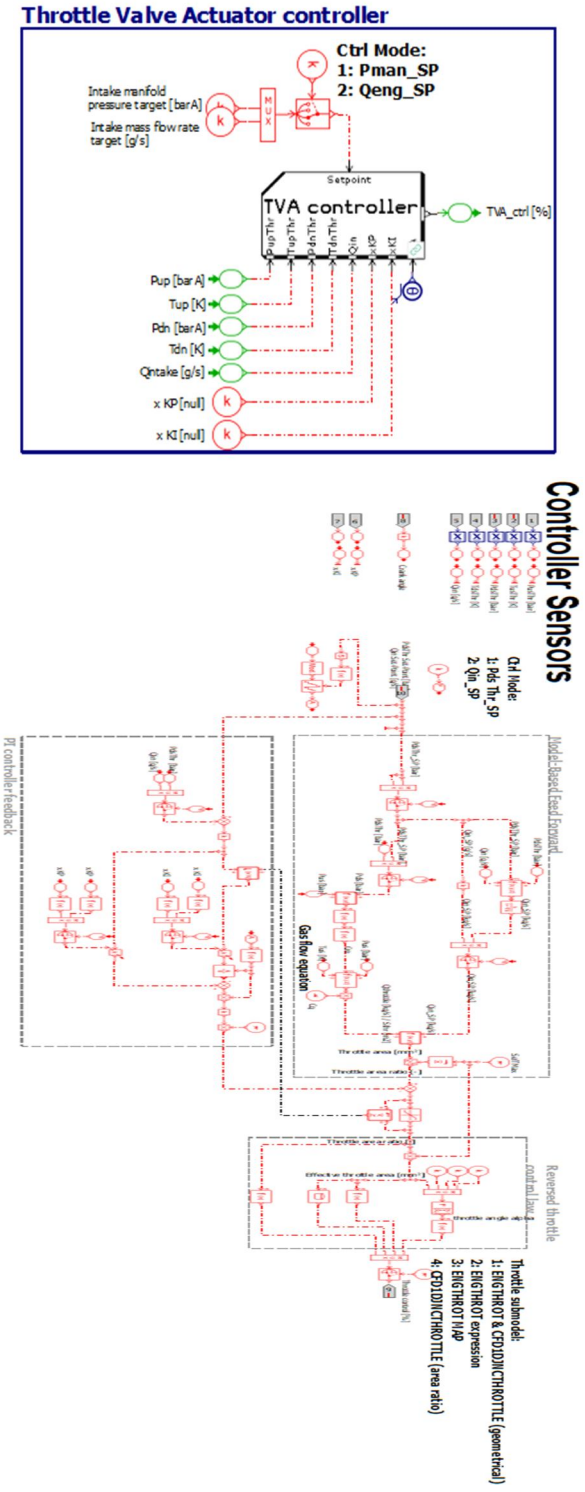



Fig (9.3): Throttle controller sub model

The turbocharger system does not model thermal behavior. Heat loss is instead included in the efficiency look-up table data. Heat transfer modelling would need a considerably higher degree of realism and thorough knowledge of the turbocharger assembly and internals. An electric motor is attached to the turbocharger shaft to imitate the electric turbocharger system. To account for the greater motor mass, the inertia is likewise increased. The figure below representations the Hybrid turbocharger in AMESim software

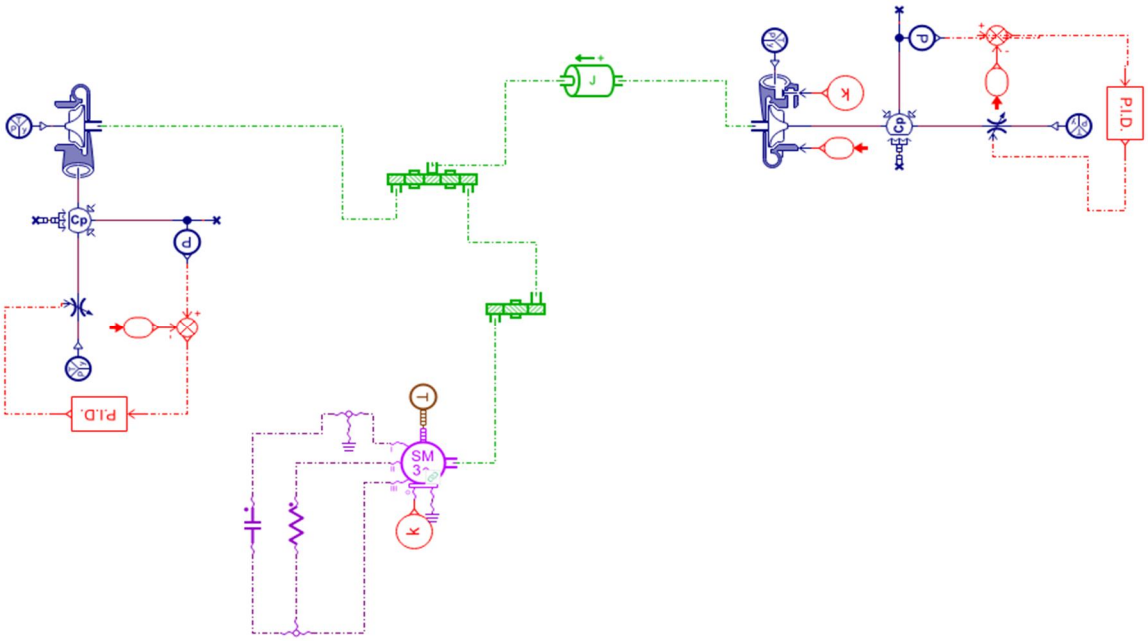



Fig (9.4): Overview of hybrid turbocharger components in AMESim software.

.

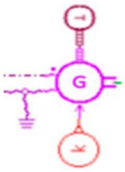
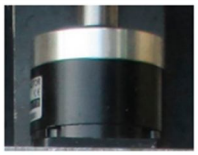
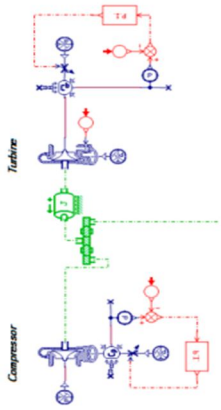
| No. | Main Component Part | Component Part in AMESim Software | Designation |
|---|---|---|---|
| 1. |  |  | electrical generator |
| 2. |  |  | PLE 120 Neugart gear ratio/1:10 |
| 3. |  |  | Turbocharger |

Table (9.1): Main components of Hybrid turbocharger.

The table includes all of the key components of the hybrid turbocharger, such as the turbocharger components, gear ratio (1:10), and 100 W electrical generator, as well as the essential symbols utilized in the AMESim simulation.

*A. Simulation of 4-cylinder conventional turbocharged engine*

AMESim software is included with a demonstration model of 4-cylinder turbocharged engine. The results from this model will be considered as results from the conventional turbocharger.

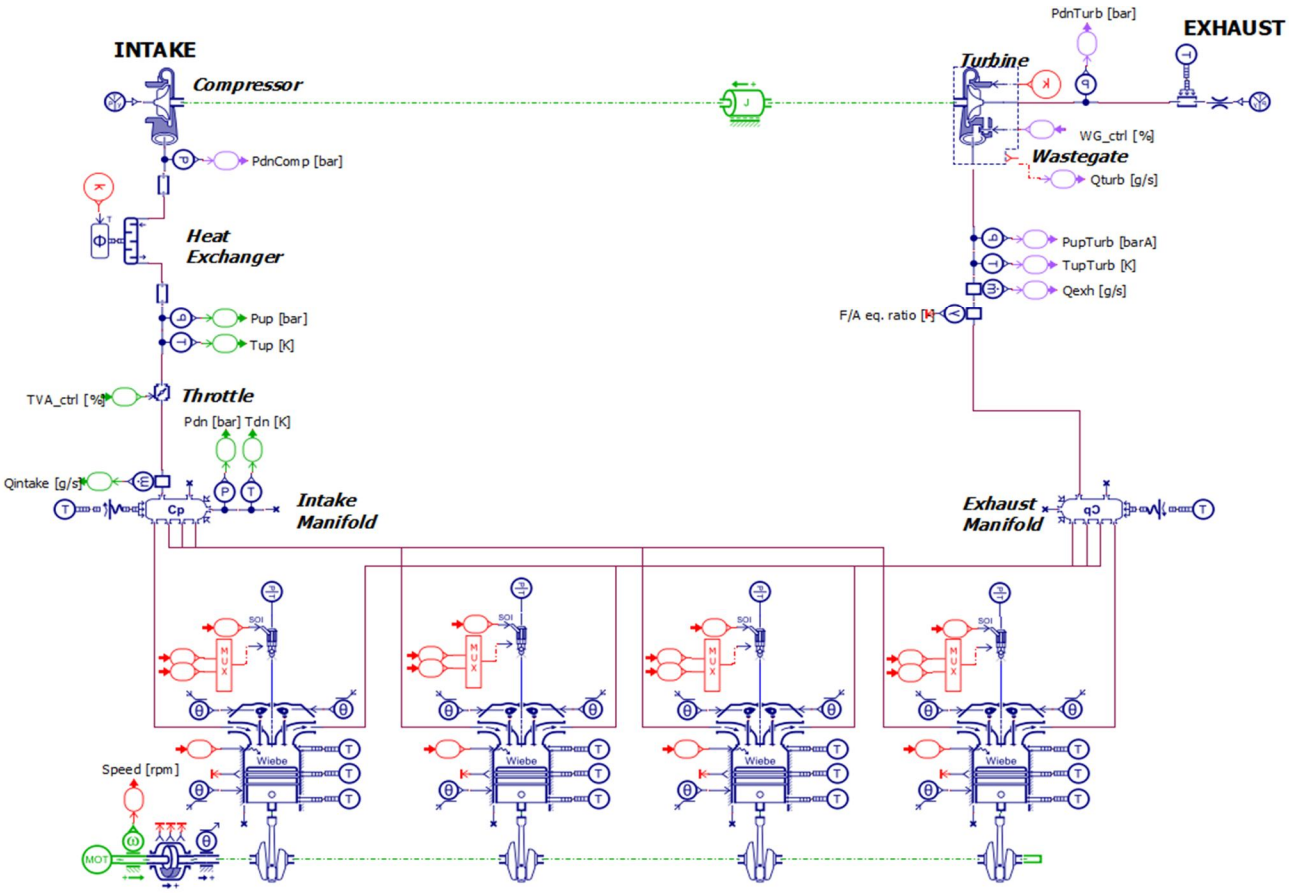



Fig (9.5): 4-cylinder conventional turbocharged engine.

We simulate the model by entering the engine specifications in the parameter tab, which yields the following results.

1) *Results from 4-cylinder conventional turbocharged engine:*The output of the turbo shaft is shown in the figure. The interval from 0-2s, the turbo shaft reaches its max speed of 110,000rpm from rest. And after 3s, due to constant pressure from the exhaust gases, the turbocharger shaft speed remains constant i.e., 110,000rpm.

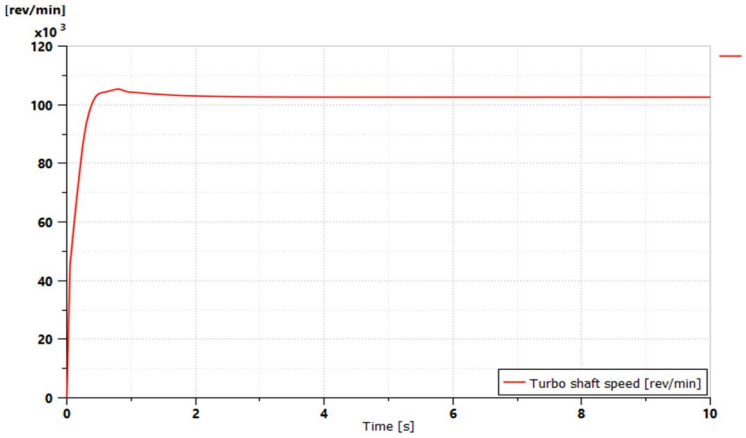



Fig (9.6): Turbocharger shaft speed (conventional TC)

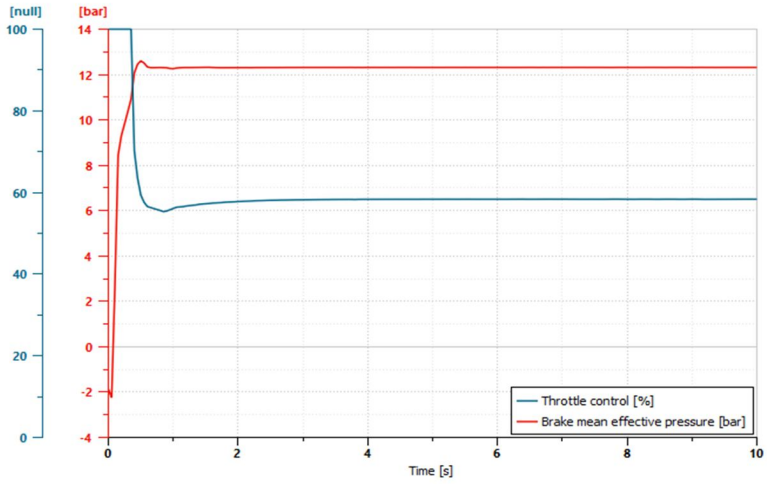



Fig (9.7.): Brake mean effective pressure of Conventional TC.

Figure illustrates the brake mean effective pressure of conventional turbocharger. The average pressure inside the engine that forces the pistons down to produce the reported torque output is shown with the throttle control in percentage.

*B. Simulation of 4-cylinder hybrid turbocharged engine*

The turbocharger shaft is connected to a motor generator, which is electrically assisted by the use of capacitor. The turbo shaft is coupled with planetary gear set having a 1:10 gear ratio.

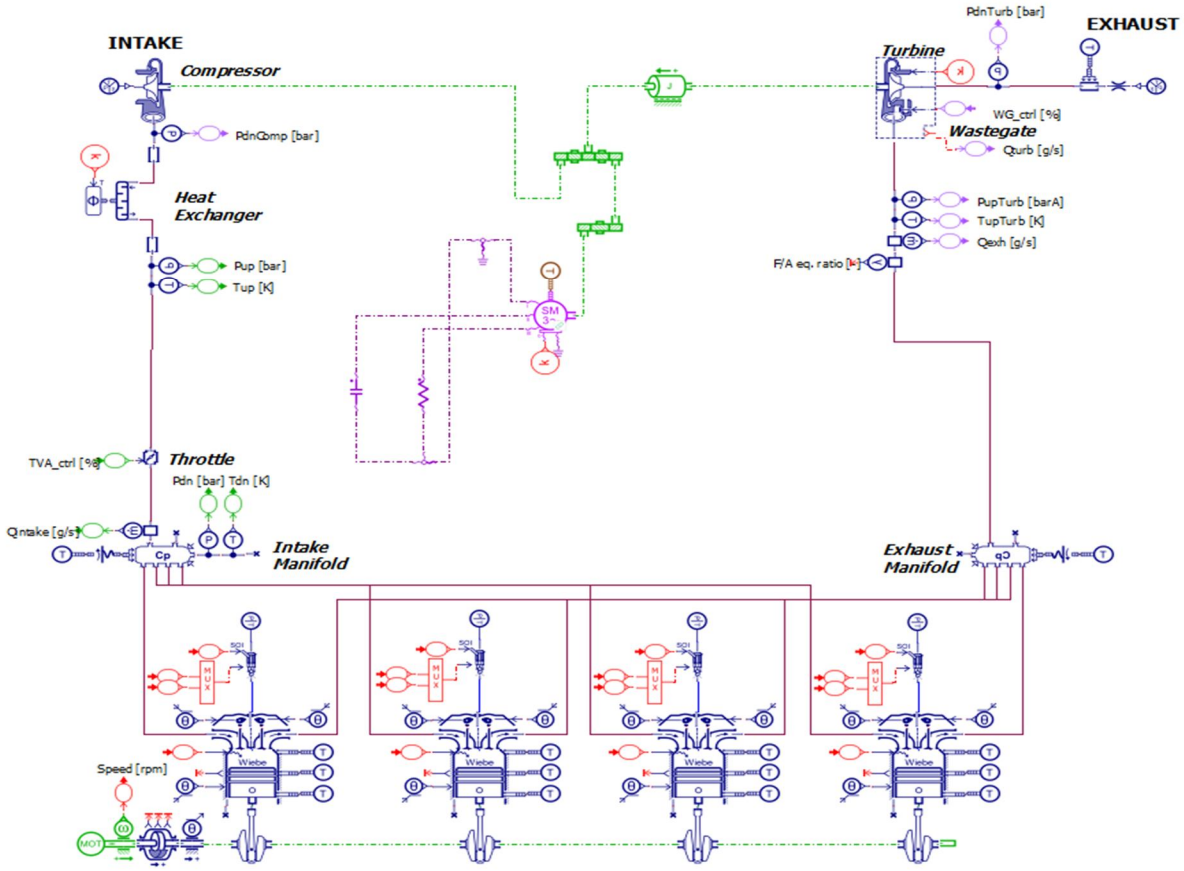



Fig (9.9):4-cylinder engine equipped with hybrid turbocharger simulated with AMESim.

As previously, we receive the following results after entering the engine specs into the model.

*1) Results from 4-cylinder hybrid turbocharged engine:*

| Evaluated Parameter | Unit of Measurement | Value of the Parameter |
|---|---|---|
| Compressed air pressure | MPa | 0.1..0.2 |
| Turbocharger shaft speed | rpm | 140,000–160,000 |
| Electric generator shaft speed | rpm | 14,000–16,000 |
| The voltage of the current generated | V | 2–23 |
| The intensity of the excitation current | A | 0.5–5 |
| Load current intensity | A | 5–30 |
| Maximum power | W | 115 |

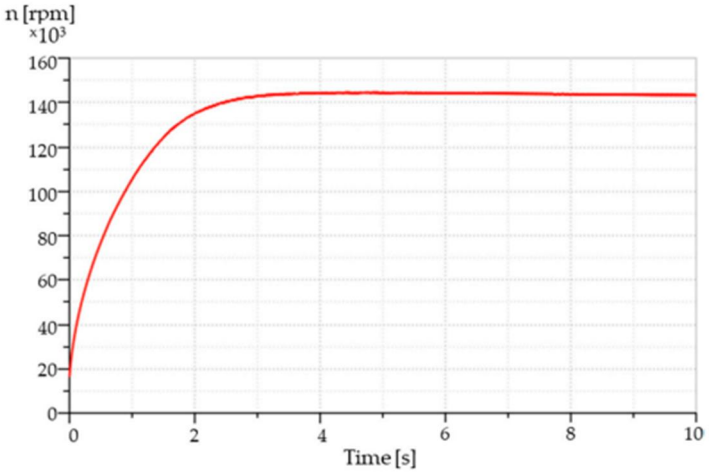



Fig (9.10): Turbocharger shaft speed (Hybrid TC)

The turbocharger shaft speed increases from 0 to 135,000rpm in the interval period between 0 and 2s. The turbocharger shaft speed remains constant at 150,000rpm after 2s due to the steady pressure of the exhaust gases.

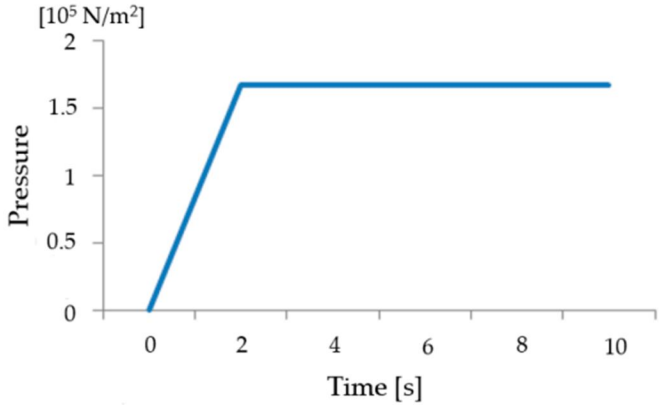



Fig (9.11): The compressor outlet pressure.

Figure shows the compressor outlet pressure with time. The experimental working value is in the range of 0 to 1.6 105 N/m2. The compressor outlet pressure increases from 0 to 1.6 105 N/m2 in the time span 0 to 2 s. The compressor output pressure stays constant at 1.6 105 N/m2 after 2 s due to the constant pressure of the exhaust gases.

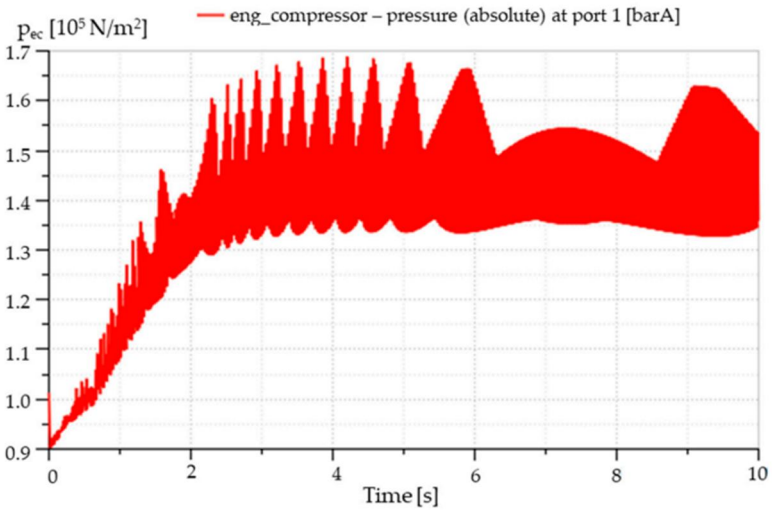



Fig (9.12): Variation of compressed air pressure.

Figure shows the compressor output pressure through time with simulation values ranging from 0 to 1.6 105 N/m2. Changeable values of the compressed air pressure can be noticed in the time interval 0–10 s.

## X. CONCLUSIONS

Designing a turbocharger is a challenging task. It needs a lot of compatibility and matching. A/R ratio is the primary selection criteria for the selection of a compressor, which is the most important part of the turbocharger. If the turbocharger is big in size, then it takes more time to spool and it the turbocharger is smaller than the specifications, then we will get a better boost experience at the starting but at high engine RPM the turbocharger will chokes the engine. Sequential turbocharger delivers same performance as a VGT with a significantly smaller engine size. Though it has a good potential considering that we can downsize an engine, but the working of a sequential turbocharger is very complicated and that's why it is not very promising. Electric turbocharging application leads to remarkable improvement at low-end torque, better engine performance and increased overall engine efficiency. Alternating between motoring and generating modes reduced fuel usage by up to 5% for driving cycles. EATC reduced the time it took to reach the optimum boost level during a load increase by up to 30%. Ti3SiC2 was discovered to be the best suitable because it is the only ternary ceramic that is easy to manufacture and requires very little lubrication and cooling.

Typical transient cases were discussed, stressing the diverse development patterns of engine attributes as well as the engine control system's needs. At the same time, the mechanism of turbocharger lag was discussed, as well as its consequences for engine responsiveness. Materials such as electric generators and gearboxes were chosen based on their practicality. We compared the output graphs of a conventional turbocharger and a hybrid turbocharger using the AMESim software. Resulting a great improvement in the transient response of the hybrid turbocharger.

## XI. ACKNOWLEDGMENT

Acknowledgement is a sweet and short way to express gratitude. I take this opportunity heartfelt thanks to all those who have guided, supported and encouraged me to complete my research work.

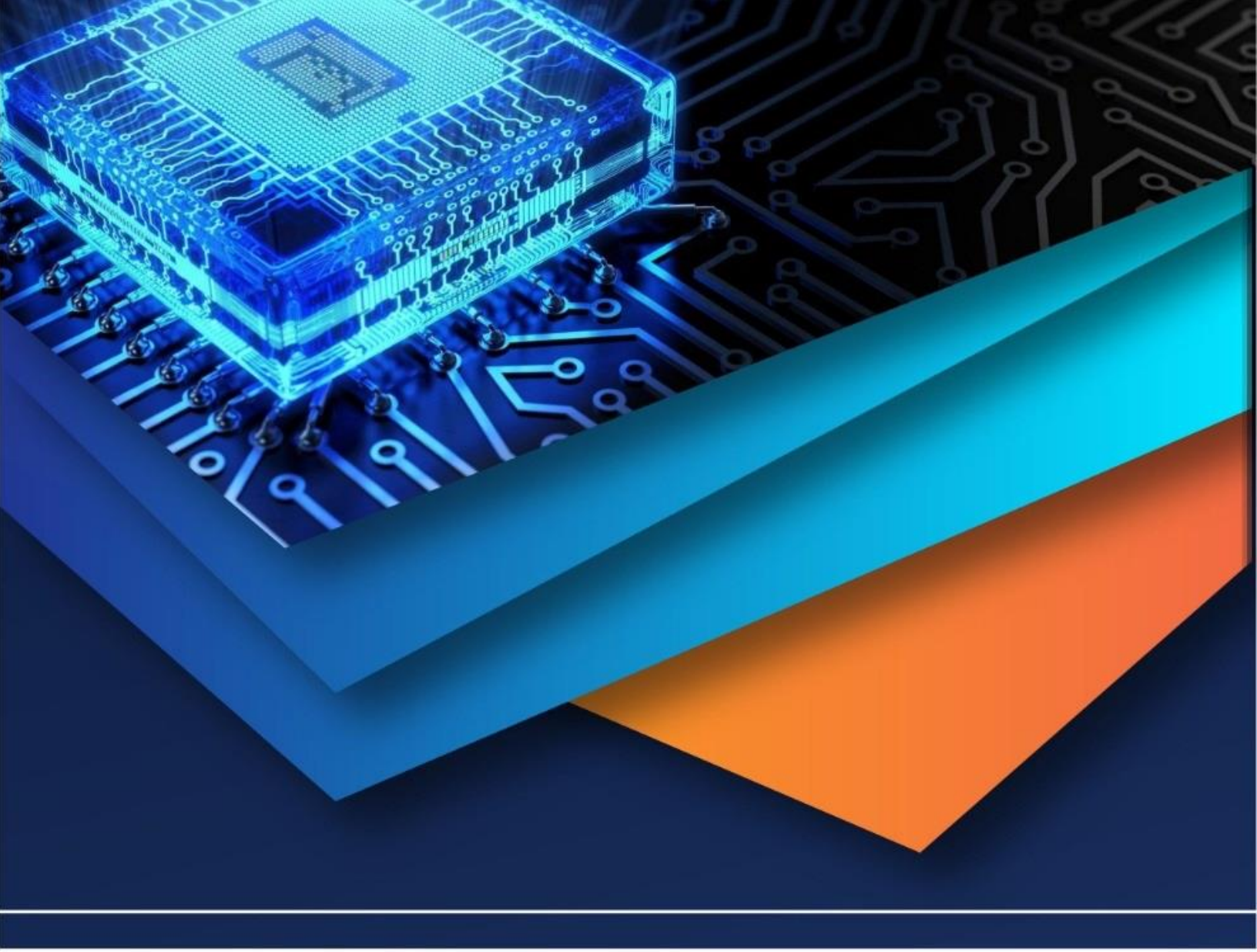
Indeed, the words at my command are not adequate to convey the depth of my feeling and gratitude to my project guide prof. Shivaji kale, for his most valuable and inspiring guidance with his friendly nature, love and affection, for his attention and magnanimous attitude right from the first day, constant encouragement, enormous help and constructive criticism throughout the course of this investigation and preparation of this manuscript. I am also thankful to prof. Prashant kavale (project coordinator), for counsel generous guidance and useful suggestions; special thanks are tendered to prof. M. B. Murugkar, head of mechanical department.Taken deep appreciation is being rendered to dr. K. N. Nandurkar, principal, k.k wagh institute of engineering education and research, nashik, for providing the facilities during the course of my studies. I would like to thank the entire staff members of mechanical department for timely help and inspiration for completion of the dissertation.

My vocabulary fails to get words expressed for my respect and sense of gratitude to my beloved parents, colleagues and friends who always wanted my success, inspired me with their love and affections and for the sacrifice made by them to shape my career.

## REFERENCES

[1] Chiriac, R.-L.; Chiru, A.; Boboc, R.G.; Kurella, U. Advanced Engine Technologies for Turbochargers Solutions. Appl. Sci. 2021, 11, 10075. https://doi.org/10.3390/app112110075
[2] Capata, R. Sciubba, E. Study, Development and Prototyping of a Novel Mild Hybrid Power Train for a City Car: Design of the Turbocharger. Appl. Sci. 2021, 11, 234. https://doi.org/10.3390/app11010234
[3] Rares-Lucian Chiriac, Anghel Chiru, NEW TECHNICAL SOLUTION FOR HYBRID TURBOCHARGERS, 24-Mar-2020.
[4] Bhavik Kumar Padhiyar, Dr.P. K. Sharma, Application of Hybrid Turbocharger to improve performance of Engine, A R DIGITECH International Journal of Engineering, Education and Technology (ARDIJEET) www.ardigitech.in ISSN 2320-883X, volume 2 issue 2, 01-Apr-2014.
[5] Nenad Raspopović, Jovan Dorić, Ivan Grujić, Nebojša Nikolić, ANALYSIS OF HYBRID TURBOCHARGER IN MOTOR VEHICLE IC ENGINE, International Congress Motor Vehicles & Motors 2018 Kragujevac, Serbia October 4th - 5th, 2018.
[6] Alin-Gabriel, D.: "Study on engine efficiency and performance improvements through hybrid turbocharging assisting", Master's thesis in Automotive Engineering, Chalmers University of Technology Gothenburg, Sweden 2014.
[7] Genetic Optimization of Turbomachinery Components using the Volute of a Transonic Centrifugal Compressor as a Case Study - Scientific Figure on ResearchGate.
[8] Gravdal, Anders Gusevik. "Diesel Engine Response Improvements using Hybrid Turbocharging." (2017).
[9] Pesyridis, Apostolos & Shettigar, Vivek. (2014). Materials Selection for Variable Geometry Turbine Nozzle for Gasoline Engine Application. Proceedings of the ASME Turbo Expo. 1. 10.1115/GT2014-27119.
[10] Syed Kamran Arshad-Ali (2015) Suitability of Hybrid Electric Powertrains with Electric Turbocharger.
[11] Constantine D. Rakopoulos • Evangelos G. Giakoumis (2009) Diesel Engine Transient Operation 10.1007/978-1-84882-375-4.
[12] Rares, -Lucian Chiriac 1, *, Anghel Chiru 1 (2021) Advanced Engine Technologies for Turbochargers Solutions https://doi.org/10.3390/app112110075
[13] www.garrettmotion.com/racing-and-performance/performance-catalog/turbo/garrett-boost-club-line-gbc17-250/

©IJRASET: All Rights are Reserved | SJ Impact Factor 7.538 | ISRA Journal Impact Factor 7.894 |



10.22214/IJRASET

45.98

IMPACT FACTOR: 7.129

IMPACT FACTOR: 7.429

# INTERNATIONAL JOURNAL FOR RESEARCH

IN APPLIED SCIENCE & ENGINEERING TECHNOLOGY

Call : 08813907089 (24*7 Support on Whatsapp)